

# Gas exchange in subarctic grasslands

Impact of medium-term and long-term soil warming on leaf gas exchange  
in subarctic *Ranunculus acris* L.

---

Timon Callebaut

**Faculty of Science, Department of Biology  
University of Antwerp**

In cooperation with the Agricultural University of Iceland

**Promotor:** Bjarni D. Sigurdsson

**Co-promotors:** Ivan Janssens, Ruth Phoebe Tchana Wandji

Master Project submitted to obtain the degree of Master in Biology,  
specialisation Global change biology

2021-2022

## Contents

Abstract aimed at scientific peers.....	4
Abstract aimed at the public at large.....	4
List of abbreviations and acronyms .....	5
1. Introduction .....	6
1.1 Climate change.....	6
1.2 Gaps in knowledge and limitations.....	7
1.3 Photosynthesis response curves.....	8
1.4 Research questions and hypotheses.....	9
2. Materials and methods .....	10
2.1 Study site.....	10
2.2 Experimental design.....	11
2.2.1 Study duration.....	12
2.2.2 Species studied .....	13
2.3 Gas exchange measurements .....	13
2.3.1 Survey measurements .....	13
2.3.2 Response curves.....	14
2.4 Handling of leaf samples.....	15
2.5 Response curve modelling and parameter calculations .....	15
2.5.1 $C_i$ response curves .....	15
2.5.2 Photosynthetic parameters .....	16
2.5.3 PAR response curves.....	17
2.6 Statistical analysis .....	18
2.6.1 Survey measurements .....	18
2.6.2 Response curves.....	18
3. Results.....	20
3.1 Survey measurements .....	20
3.2 Photosynthesis response curves.....	25
3.2.1 A/ $C_i$ convexity parameters.....	25
3.2.2 A/ $C_i$ Farquhar parameters .....	26
3.2.3 A/I convexity parameters.....	26
3.3 C/N, stable isotopes and SLA .....	35
4. Discussion.....	37
4.1 Effect of increasing soil temperature on photosynthesis.....	37

4.1.1 Previous studies .....	37
4.2 Effect of duration of soil warming on photosynthesis.....	39
4.2.1 Previous studies .....	40
4.3 Effect of plant nitrogen status .....	40
4.4 On the dynamicity of geothermal hotspots.....	41
4.5 Limits of the project and discussion of different soil warming experiments .....	42
4.6 Importance for the future of the Arctic .....	42
5. Conclusion.....	43
Acknowledgements.....	43
References .....	44
Addendum 1: Theory on photosynthesis.....	50
Addendum 2: graphs.....	53
Addendum 3: Survey measurement protocol .....	54
Addendum 4: Response curve protocol.....	56

## Abstract aimed at scientific peers

In a future where warming is expected to reach +2-8°C at high northern latitudes, it is vitally important to understand the impact this warming will have on local ecosystems, especially under long-term warming. Little research has been done on the effects of warming on subarctic grasslands, even less focusing on photosynthesis and none at all investigating its long-term effects. This research analysed the effects of soil warming, as well as its medium- (13 years) and long-term effects (>60 years) on photosynthesis of *Ranunculus acris* on two ForHot sites in the natural geothermal area near Hveragerði, Iceland. First, survey measurements were done (n = 60), recording net, saturated and maximal photosynthesis ( $A_{net}$ ,  $A_{sat}$  and  $A_{max}$ , respectively). Subsequently, light and carbon response curve measurements were taken (n = 54), providing in-depth insight into various photosynthetic mechanisms. With these measurements, the effect of a) degree of soil warming and b) duration of soil warming on photosynthesis was investigated. Results showed little to no effect of soil warming on plant productivity. While there were some differences between sites and thus duration of warming, most of these differences could be explained by covariance of leaf nitrogen content. This study suggests that, as soils continually warm due to global change, there will be no warming-induced increases in plant productivity to offset the increasing emissions of soil carbon stocks in subarctic grasslands. Future research into the effects of warming on this ecosystem should look to include air temperature warming and, ideally, other global warming drivers and effects such as carbon fertilisation or drought.

## Abstract aimed at the public at large

For the past several decades, scientists have been working to understand the exact effects of climate change on natural ecosystems worldwide. As of 2022, there are still many ecosystems about which little is known. In Hveragerði, Iceland, also known as ‘the Earthquake Town’ and ‘the Hot Spring Town’ due to the active geological and geothermal forces, an excellent opportunity presents itself to figure out what warming may do to these grasslands in the future. The ForHot project is a research site combining many different disciplines, ranging from geology to ecology, all centered around two of these geothermal hotspots near Hveragerði. One site has been heated for centuries, even occurring in Icelandic folk tales, while the other valley only became heated in 2008, when a massive earthquake shook Hveragerði to its core. This thesis looks into the effects of warming, as well as any possible changes between the two sites with their different durations of warming.

One way in which change may present itself is in photosynthesis, the system through which plants use CO<sub>2</sub> in the air to make sugars and other plant materials. This is important, as photosynthesis by many plants worldwide is a vital way to slow the increase of global temperature. This study suggests that, contrary to expectations, plants do not become more productive in warmer soils, which has negative impacts on how much CO<sub>2</sub> will be taken up and emitted in subarctic grasslands.

## List of abbreviations and acronyms

<b>A</b>	Assimilation rate (in $\mu\text{mol m}^{-2} \text{s}^{-1}$ ).
<b>A at Ca = 400 ppm</b>	Maximal rate of photosynthesis at ambient carbon and light saturating conditions. Similar to $A_{\text{sat}}$ but for response curves (in $\mu\text{mol m}^{-2} \text{s}^{-1}$ ).
<b>A at Ci = 400 ppm</b>	Assimilation rate at an intracellular CO <sub>2</sub> of 400 ppm (in $\mu\text{mol m}^{-2} \text{s}^{-1}$ ). Needed for calculating Ls, does not have a biological meaning.
<b>A/Ci</b>	Response curve of photosynthesis over a range of Ci.
<b>A/I</b>	Response curve of photosynthesis over a range of PAR.
<b>A<sub>max</sub></b>	Maximal rate of photosynthesis at carbon and light saturating conditions (in $\mu\text{mol m}^{-2} \text{s}^{-1}$ ).
<b>A<sub>max_Ci</sub></b>	$A_{\text{max}}$ obtained from A/Ci response curves (in $\mu\text{mol m}^{-2} \text{s}^{-1}$ ).
<b>A<sub>max_I</sub></b>	$A_{\text{max}}$ obtained from A/I response curves (in $\mu\text{mol m}^{-2} \text{s}^{-1}$ ).
<b>AQY</b>	Apparent quantum yield; initial slope of A/I curve.
<b>A<sub>sat</sub></b>	Maximal rate of photosynthesis at ambient carbon and light saturating conditions (in $\mu\text{mol m}^{-2} \text{s}^{-1}$ ).
<b>Ca</b>	Atmospheric carbon dioxide (in ppm).
<b>CCP</b>	Carbon compensation point (in ppm).
<b>Ci</b>	Intracellular carbon dioxide (in ppm).
<b>Ci at Ca = 400 ppm</b>	Intracellular CO <sub>2</sub> concentration at atmospheric CO <sub>2</sub> concentration (in ppm).
<b>CSP</b>	Carbon saturation point (in ppm).
<b>GN</b>	Grassland New, the site experiencing medium-term soil warming.
<b>GO</b>	Grassland Old, the site experiencing long-term soil warming.
<b>gsw</b>	Stomatal conductance to water vapour (in $\mu\text{mol m}^{-2} \text{s}^{-1}$ ).
<b>J<sub>max</sub></b>	Maximum rate of photosynthetic electron transport (in $\mu\text{mol m}^{-2} \text{s}^{-1}$ ).
<b>LCP</b>	Light compensation point (in $\mu\text{mol m}^{-2} \text{s}^{-1}$ ).
<b>Ls</b>	Relative stomatal limitation (in %).
<b>LSP</b>	Light saturation point (in $\mu\text{mol m}^{-2} \text{s}^{-1}$ ).
<b>N%</b>	Leaf nitrogen content (in %).
<b>R<sub>d</sub></b>	Mitochondrial respiration in non-photorespiratory processes (in $\mu\text{mol m}^{-2} \text{s}^{-1}$ ).
<b>R<sub>dark</sub></b>	Dark respiration (in $\mu\text{mol m}^{-2} \text{s}^{-1}$ ).
<b>SE</b>	Standard error.
<b>Tsoil</b>	Soil temperature (in °C).
<b>V<sub>Cmax</sub></b>	Maximum rate of Rubisco carboxylase activity (in $\mu\text{mol m}^{-2} \text{s}^{-1}$ ).
<b>α</b>	Initial slope of A/Ci curve.
<b>θ</b>	Convexity parameter of A/Ci or A/I curve.

# 1. Introduction

## 1.1 Climate change

Anthropogenic global change is overwhelmingly supported within the scientific community (Fig. 1) (IPCC, 2021). Human-induced climate change impacts include increasing frequency of weather extremes such as heat waves, droughts and floods (Stott, 2016), ocean acidification (Chen et al., 2017) and rising sea levels due to thermal expansion of water (Kuhlbrodt & Gregory, 2012) and melting of land ice caps (Sharp et al., 2011) and glaciers (Colucci & Guglielmi, 2019). These impacts are set off either by the rapid increase in atmospheric greenhouse gasses or by the resulting increase in air temperature (Meinhausen et al., 2009). However, due to the complexity of the issue, many of the specific, small-scale processes and mechanisms of global change are as yet unknown, despite ever-increasing scientific interest in the last thirty decades (e.g. Abdelrahman et al., 2020; Jansson & Hofmockel, 2019).

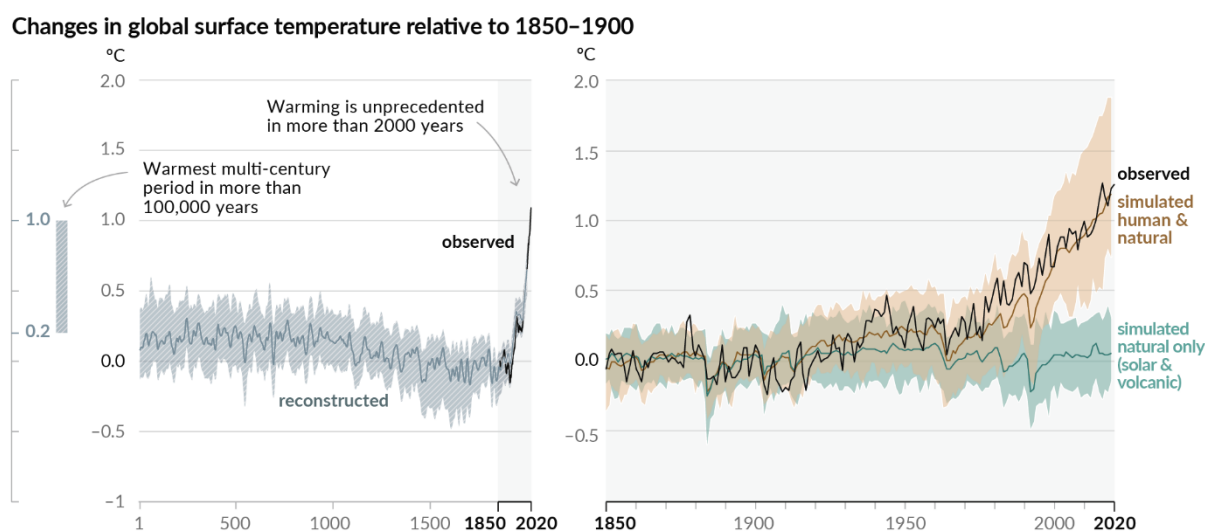


*Fig. 1: Climate warming rates over the last 2000 years; a) change in global surface temperature (decadal average) as reconstructed (1-2000) and observed (1850-2020), b) change in global surface temperature (annual average) as observed and simulated using human & natural and only natural factors. (IPCC, 2021)*

Global temperatures have increased by about 1.2°C above pre-industrial levels (GISTEMP team, 2021; Lenssen et al., 2019), with warming expected to last until at least the mid-century. Unless significant reductions in greenhouse gas emissions occur in the coming decades, the global mean temperature is predicted to increase by 2.6-4.8°C by the end of the century and even more toward the poles (2-8°C) (IPCC, 2022). Additionally, actual global change may occur at a faster pace than models indicate (Chen et al., 2017; Van Oldenbough et al., 2009; Xu et al., 2018).

This environmental change will have a significant and lasting effect on plants, mostly due to changes in temperature and precipitation (Matesanz and Valladares, 2014). The exact effects of climate change on plants are still not entirely known, but an increase in research into the effects of warming on plants in recent years have shown changes in ecophysiology (Huan et al., 2012; N6ia J6nior et al., 2018), phenology (Leblans et al., 2017), biomass production (Dieleman et al., 2012), metabolome (Gargallo-Garriga et al., 2017), species composition (Wang et al., 2012) and carbon allocation to mycorrhizal symbionts (Hawkes et al., 2007).

## 1.2 Gaps in knowledge and limitations

Long-term warming experiments, including SPRUCE (McPartland et al., 2020) and B4WarmED (Jamieson et al., 2015) in North America and the TRACE project in Puerto Rico, are being increasingly set up to study warming effects, often coupling warming with other global change factors such as elevated CO<sub>2</sub>. However, one significant limitation of most experimental ecological warming projects is the short time scale in which they are run, which is usually <10 years (e.g. TRACE, SPRUCE) to <20 years (e.g. B4WarmED). In fact, the longest running soil warming study was only set up in 1991 (Harvard Forest LTER). Additionally, despite the amplified warming towards the poles, there are few studies that focus on subarctic ecosystems, one notable exception being the Abisko experiment, which uses open-top chambers to induce passive warming (Marion et al., 1997). Furthermore, while photosynthesis is a widely accepted proxy for plant fitness (Heckmann et al., 2013), there are no papers in circulation that focus on photosynthesis measurements in these warming experiments.

ForHot/FutureArctic is an interdisciplinary research project near Hverager6i, Iceland allowing soil warming experiments on grasslands across a wide ecological range (Fig. 2) (e.g. De Gruyter et al., 2020; Gargallo-Garriga et al., 2021; Kutcherov et al., 2020, Sigurdsson et al., 2016). The project site in Iceland is in the perfect position to develop knowledge on the long-term response of subarctic grasslands to warming due to its volcanic hotspots that have created temperature gradients in grasslands that span up to >60 years.

One might raise the concern that climate change will not just affect the temperature of the soil but also that of the air. While not perfect, the ForHot site with its long-lasting soil warming is in fact a good proxy for climate change, as the dense grassland canopy traps radiation heat from the soil, effectively heating both the air and plants up to the leaf level.

The subarctic grassland is dominated by *Ranunculus acris* L., *Agrostis capillaris* L. and *Equisetum pratense* Ehrh., making these the ideal target species for studying the impact of warming on plants in

this ecosystem. Due to time constraints, the decision was made for this research project to focus on the photosynthesis of the  $C_3$  dicotyledon *R. acris*. More details about the research site follow in the Methodology section.

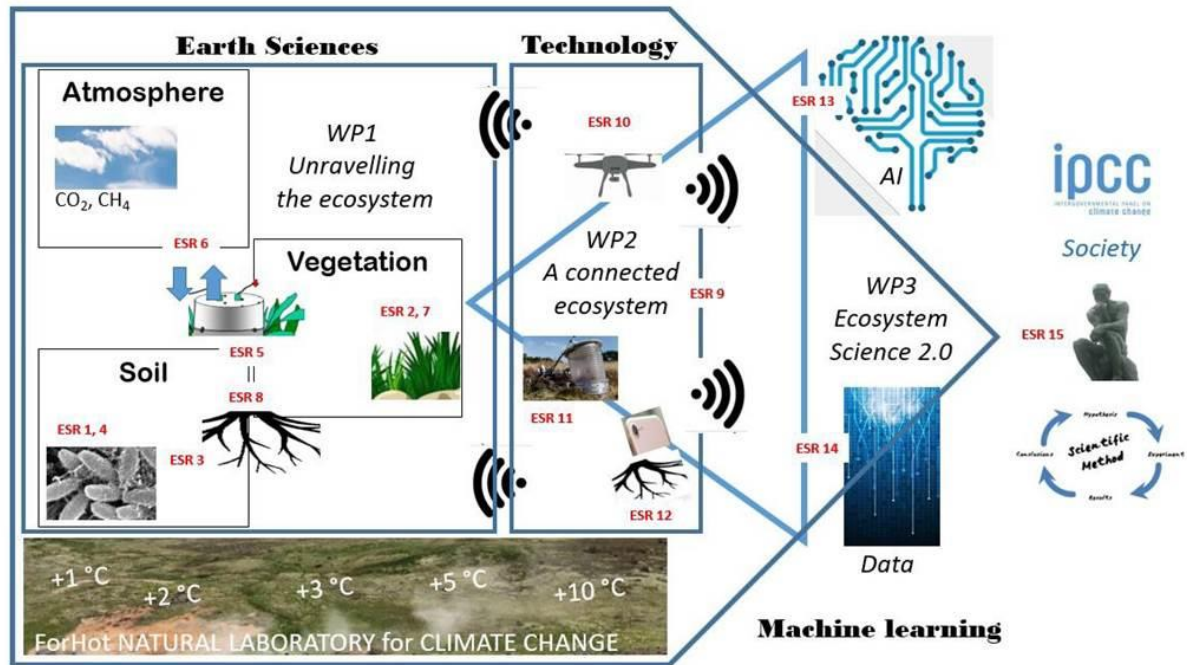


Fig. 2: Overview of current projects by FutureArctic, an interdisciplinary team of PhD researchers on the ForHot site. This project falls under vegetation (ESR 7). Figure courtesy of FutureArctic: <https://www.futurearctic.be/the-project/>

### 1.3 Photosynthesis response curves

The biochemical process of photosynthesis has been extensively studied. While an overview thereof is very relevant for this thesis, including it here would make the introduction very long. Therefore, an in-depth summary of the relevant theory is presented in Addendum 1.

There are multiple ways to record and derive meaning from photosynthesis measurements. One established method, utilised in this experiment, makes use of response curves. Response curves allow for measuring plant assimilation rate reactions to changes in one single driving factor. From these resulting curves, a number of insightful parameters can be extracted that shed light on photosynthetic capacity and dark respiration, as well as on their responses to changing environmental conditions. In this experiment, response curves to changes in intracellular carbon (Ci) and in light (PAR) were studied.

## 1.4 Research questions and hypotheses

This research aims to fill gaps in knowledge on photosynthesis responses to warming in subarctic grasslands by seeking to answer the following research questions:

1. What is the effect of increasing soil temperature on assimilation rate in *Ranunculus acris* in subarctic grasslands?
2. Are these effects the same when comparing plant communities exposed to long-term (>60 years) with medium-term (13 years) soil warming?

The hypothesis behind the first research question is that plants growing in warmer plots exhibit a higher assimilation rate, given the established positive relation between temperature and photosynthesis rate, up to the optimum maximum temperature (Fig. 3). Similarly, soil microbes grow faster and exhibit greater activity in increased temperature (FdZ-Polanco et al., 1994, Walker et al., 2018). The resulting accelerated mineralisation of soil organic matter can be expected to alleviate nutrient limitations on photosynthesis (mainly nitrogen), and thus exacerbate the increase of photosynthesis under warmer soil conditions. The warmed plots studied in this experiment do not exceed the optimum temperatures of either plants or soil microbes. As such, the hypothesis is that warmed plots exhibit greater photosynthetic assimilation rates than ambient plots.

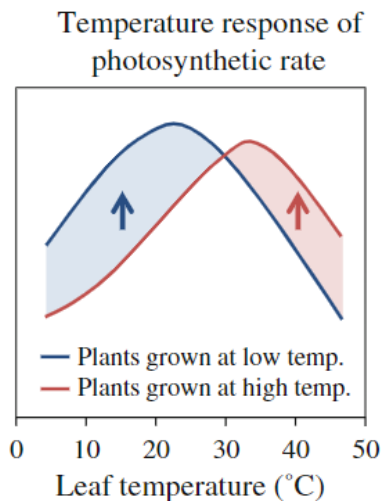


Fig. 3: Idealised theoretical diagram of the response of assimilation to temperature, with different optima for low- and high-temperature acclimatised plants. (Yamori et al., 2014)

The hypothesis linked to the second research question is that plants living in long-term warmed plots have higher assimilation rate than plants in medium-term warmed plots. Like all organisms, plants require time to adjust to changes. *R. acris* is a perennial plant, with a potential lifespan of >15 years. The hypothesis that is being tested is that plants experiencing long-term soil warming have experienced these conditions throughout their entire life and as such had sufficient time to adapt or acclimatise to the increased temperature, while this is not yet the case for plants in medium-term soil warming.

## 2. Materials and methods

### 2.1 Study site

The experiment was conducted in the Hengill thermal area near the village of Hveragerði in South Iceland (64.008°N, 21.178°W; 83-168 m above sea level; Fig. 4), approximately 40 km east of Reykjavik. The geothermal activity at the study site, which is mainly expressed through hot springs and fumaroles, is caused by the Hengill volcanic system being an intersection of Hengill, Hrómundartindur and Hveragerði volcanic zones (Gargallo-Garriga et al., 2021).

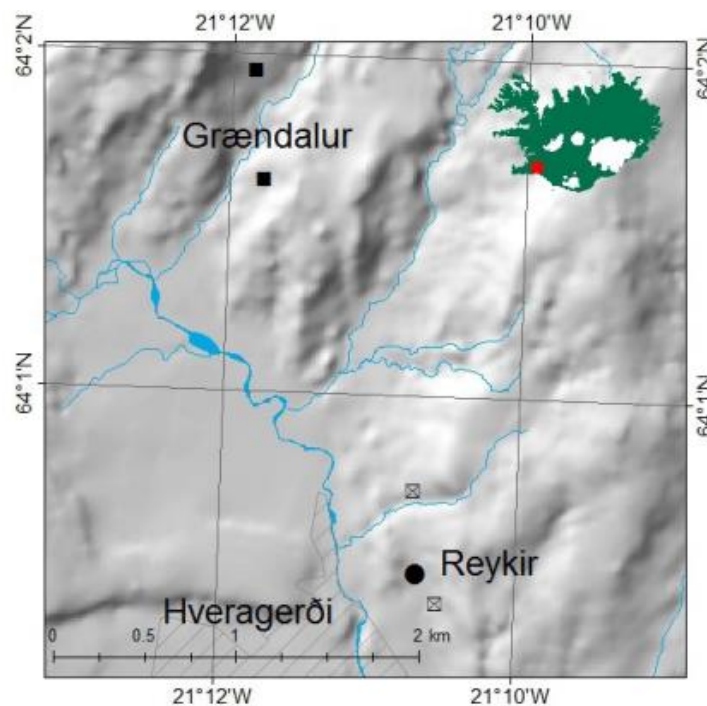
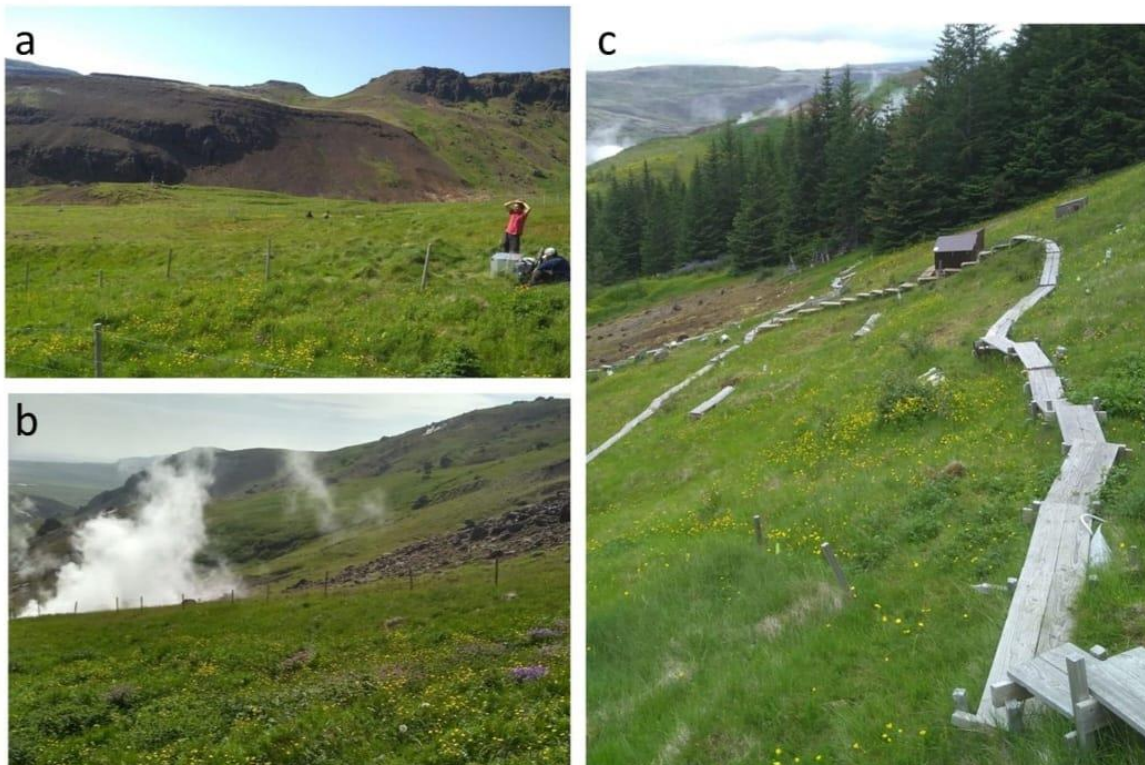


Fig. 4: location of study sites GO (squares) and GN (circle) in South Iceland (Figure courtesy of Sigurdsson et al., 2016).

Two separate sites were studied, both consisting of grassland over a Brown Andosol, dominated by *Agrostis capillaris*, *Ranunculus acris* and *Equisetum pratense*. Geothermal activity at the first site, Grassland Old (GO, Figs. 4 and 5a-b), was already reported in Icelandic sagas – it was coined *the green valley* because the warmed soils kept the vegetation green much longer – and has thus been geothermically active for centuries (Zakharova & Spichak, 2012). While it should be noted that geothermal activity is often dynamic in nature (Carotenuto et al., 2016), the area's distribution of hotspots and geothermal vents was unchanged at least between when Kristjánsson first mapped it in 1963-1965 and when it was surveyed by Þorbjörnsson et al. (2009). Based on this, it can be assumed that the geothermal hotspots at GO have existed unchanged for at least 60 years, but probably many centuries (Sigurdsson et al., 2016). The present vegetation can therefore be assumed to have adapted

or acclimated to the increased soil temperature. The second site, Grassland New (GN, Figs. 4 and 5c), is located some kilometers southwards, where an earthquake that shook Hveragerði in 2008 caused an interesting change in geothermal activity. Whilst GO remained unchanged post-2008, the area around GN became geothermally active where before there was no warming. This onset of geothermal activity was due to the earthquake that altered the compactness of the underlying bedrock and created connective pathways for hot water to rise from below the bedrock to the surface (Halldórsson & Sigbjörnsson, 2009).



*Fig. 5: Photographs of sites GO (a-b) and GN (c).*

The sites with their remarkable differences between long-term (GO) and medium-term soil warming (GN) have sparked a proliferation of multidisciplinary research, assembled in the research projects ForHot ([forhot.is](http://forhot.is)) and FutureArctic ([www.futurearctic.be](http://www.futurearctic.be)), linked to the University of Antwerp and the Agricultural University of Iceland, among other European universities (e.g. Gargallo-Garriga et al., 2017; Leblans et al., 2017; Walker et al., 2020).

## 2.2 Experimental design

At both GO and GN, 30 long-term monitoring plots of 2 x 2 m were established along five transects each perpendicular to a geothermal hotspot, thus six plots per transect, covering a gradient in soil

temperature. The plots per transect were named a through f, with an average relative warming of +0 (control), +0.4, +1.7, +2.7, +4.6 and +10.5°C for a, b, c, d, e and f, respectively for GO and +0, +0.3, +1.7, +3.0, +8.5 and +19.8°C respectively for GN (five-yearly average soil temperature at 10 cm depth of 2017-2021, data recorded by Páll Sigurðsson; Fig. 6). The differences in soil temperature between sites are accounted for in the models used. In the survey measurements all thirty plots were sampled, the response curve measurements were limited to plots a and e.

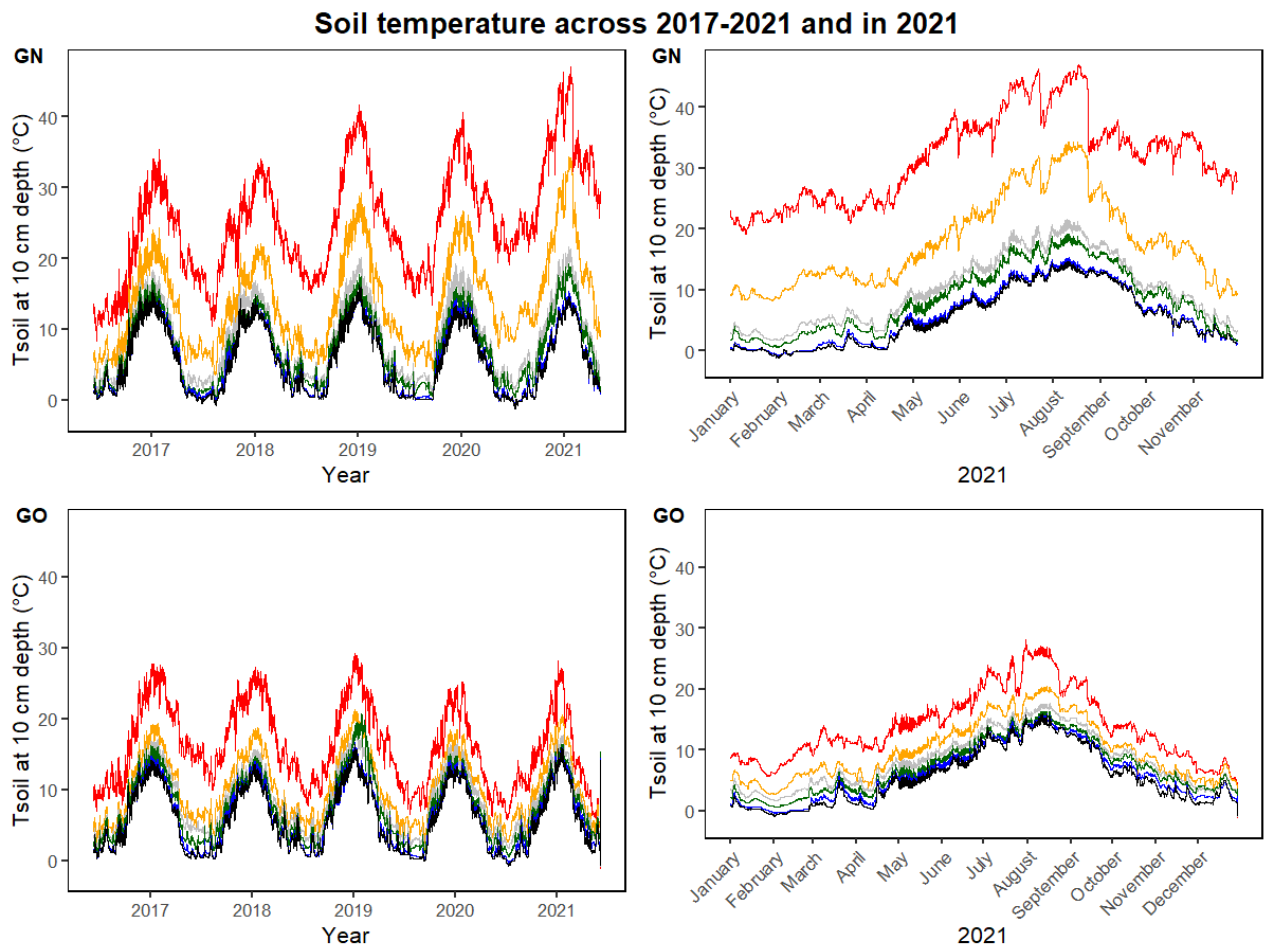


*Fig. 6: Changes in daily mean soil temperature at 10 cm depth in the six warming levels (A-F) of GN (top) and GO (bottom). Warming levels are a (control; black), b (blue), c (green), d (grey), e (orange) and f (red), from the period 2017-2021 (left) and for the year 2021 (right). (Self-made graphs, based on unpublished soil temperature data courtesy of Páll Sigurðsson).*

### 2.2.1 Study duration

Gas exchange data was taken in July and August of 2021 capturing the peak of the growing season, which normally starts in late May and ends in late August (Fig. 7) (Sigurdsson et al., 2016).

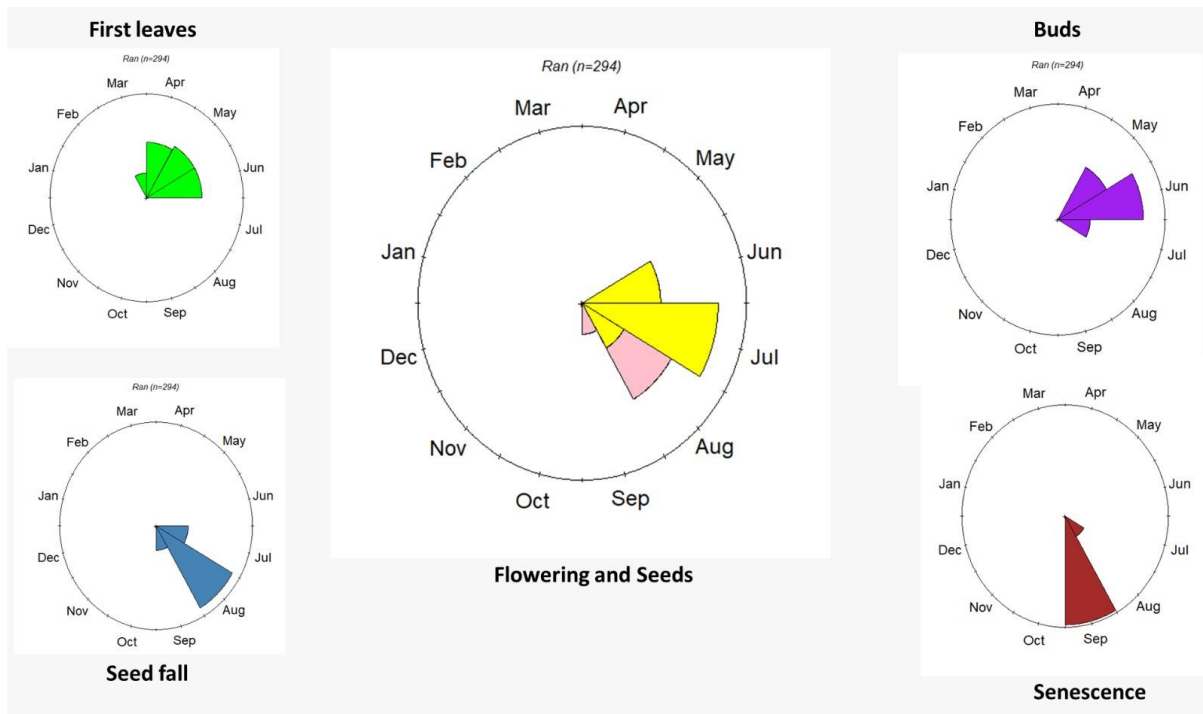


Fig. 7: Phenology traits of *R. acris* ( $n = 294$ ) in the growing season of 2021 (Unpublished data, figure courtesy of Ruth Phoebe Tchana Wandji).

Due to the highly water sensitive nature of the LI-COR gas exchange device, data could only be recorded on rain-free days. The rainy nature of Icelandic summers, with an average of 13.2 and 14.0 days of rain (>1 mm) in July and August respectively, with an additional 4.8 and 4.5 days of light to heavy drizzle (<1 mm) (Icelandic Met Office, 2012), severely limited the amount of days on which measurements could be made. Therefore the decision was made to restrict the number of plant species studied to one and also restrict the number of warming treatments to be compared to two, a and e.

### 2.2.2 Species studied

Due to the time constraints explained above, the research was conducted only on *Ranunculus acris*, a  $C_3$  dicotyledon. Along with *Agrostis capillaris* and *Equisetum pratense*, this species dominates the Icelandic subarctic grassland ecosystem (Sigurdsson et al., 2016). The species is native across Eurasia, but has also been introduced in New-Zealand and North America. Its wide distribution area makes it an interesting and widely studied species (e.g. Bourdot et al., 2013; Sarukhan & Gadgil, 1974).

## 2.3 Gas exchange measurements

### 2.3.1 Survey measurements

Using an LI-6800 Portable Photosynthesis System (Li-COR Biosciences) with a 6 x 6 cm leaf chamber and 6 x 6 cm light source, gas exchange measurements were taken on healthy, mature *R. acris* leaves.

In the first phase, between July 17-18, a one-time measurement of photosynthesis and stomatal conductance ( $g_{sw}$ ) was taken in all 30 plots at both sites. In every plot, the net photosynthesis ( $A_{net}$ ) and stomatal conductance ( $g_{sw_{net}}$ ) at the ambient light ( $A_{net}$ ) at 20°C were measured for one *R. acris* plant, followed by measurement of light saturated (at 2000  $\mu\text{mol m}^{-2} \text{s}^{-1}$  PAR) photosynthetic rate ( $A_{sat}$ ) at the ambient atmospheric carbon dioxide ( $\text{CO}_2$ ) concentration and saturating light and lastly the maximal photosynthetic rate ( $A_{max}$ ) at saturating light and atmospheric  $\text{CO}_2$  concentration (1500  $\mu\text{mol mol}^{-1}$ ) was measured.

Measurements of  $g_{sw_{net}}$  and  $A_{net}$  were taken as soon the system had stabilized following the clamp-on (typically < 1 min), after which the  $A_{sat}$  and  $A_{max}$  measurements were taken. This happened after the photosynthetic rate had stabilized in the changed PAR and  $\text{CO}_2$ , which was typically after ca. 3-4 min and 4-6 min, respectively. To get comparable data for GN and GO and for the different temperature levels, the measurements were taken on subsequent days and the conditions in the cuvette were standardised: air temperature was kept at 20°C and vapor pressure deficit (VPD) at 1.1 kPa. It should be noted that as these measurements took two days to finalize, the ambient weather conditions varied somewhat. The protocol constructed for survey measurements is supplied in Addendum 3.

### 2.3.2 Response curves

In the second phase of the project, response curves were obtained in plots a and e of the first three transects at both sites for 4-5 plants in each plot (biological replicates). Before the response curves were initiated the leaves were enclosed in the cuvette at saturating light (2000  $\mu\text{mol photons m}^{-2} \text{s}^{-1}$  PAR) and low  $\text{CO}_2$  concentration (30  $\mu\text{mol mol}^{-1}$ ), at 20°C air temperature. It typically took 4-6 min before the photosynthesis had reached steady state in the new conditions. Then, for the A/Ci curves, light-saturated photosynthetic rate was recorded at eight different atmospheric  $\text{CO}_2$  concentrations starting at low concentration and ending at saturating concentrations (30, 100, 200, 300, 400, 700, 1000 and 1500  $\mu\text{mol mol}^{-1}$ ).

Afterwards, A/I curves were obtained. Carbon concentration was kept at a saturating level (1500  $\mu\text{mol mol}^{-1}$ ) as assimilation rates were obtained at eight light concentrations (2000, 1250, 1000, 750, 500, 250, 100, 50 and 0  $\mu\text{mol photons m}^{-2} \text{s}^{-1}$ ). All measurements of both response curves were taken over a combined duration of approximately one hour. The protocol constructed for response curve measurements is supplied in Addendum 4.

All leaves that were used in survey or response curve measurements were collected, the area was scanned using a WinSEEDLE 5.1a leaf scanner (Regent Instruments Inc., Canada) and stored at -18°C until further processing.

## 2.4 Handling of leaf samples

In late August, after all field measurements were taken, the leaf samples were processed in the lab. First, they were dried at 40°C for two days in order not to degrade biochemical systems, after which their dry biomass was weighed. From the leaf area and dry weight, the specific leaf area was calculated. Next, the leaves were ground to a fine powder using a porcelain mortar and pestle. The samples were then sent to a lab at the Department of Geology, University of Tartu, Estonia, where carbon (C) and nitrogen (N) contents were measured. Additionally, a  $\delta^{15}\text{N}$  and  $\delta^{13}\text{C}$  isotope analysis was performed. After the C/N analysis, a second thorough drying was done at 105°C.

## 2.5 Response curve modelling and parameter calculations

### 2.5.1 $C_i$ response curves

In assimilation rate – intracellular carbon ( $A/C_i$ ) response curves, assimilation rates are measured at a range of  $\text{CO}_2$  concentrations, while light is kept at a saturating level and other factors such as cuvette temperature and VPD are kept stable. The resulting curve can be fitted to the model developed by Farquhar, von Caemmerer and Berry (Farquhar et al., 1980). Generally, this model follows the equation

$$A_{net} = \min(A_c, A_j) - R_d \quad (1)$$

where  $A_{net}$  is the measured net assimilation rate,  $A_c$  is the gross assimilation rate when Rubisco activity is limiting,  $A_j$  the gross assimilation rate when RuBP-regeneration is limiting, and  $R_d$  is the rate of dark respiration (Fig. 8a).

In this equation,  $A_c$  and  $A_j$  are non-linear functions of chloroplastic  $\text{CO}_2$  concentration ( $C_c$ ), which can be difficult to estimate using portable instruments. In the event that  $C_c$  is not available, it is customary to use intercellular  $\text{CO}_2$  concentration instead.

Fitting the model requires an investment of time, as the transition point has to be manually specified in every curve measurement. As a solution to this problem, Duursma (2015) proposed utilising a hyperbolic minimum equation, mirroring the convexity formula (Roberntz & Stockfors, 1998), which avoids a discontinuity:

$$A_m = \frac{A_c + A_j - \sqrt{(A_c + A_j)^2 - 4\theta A_c A_j}}{2\theta} - R_d \quad (2)$$

where  $\theta$  is a shape parameter, and  $A_m$  is the hyperbolic minimum of  $A_c$  and  $A_j$  (Fig. 8b).

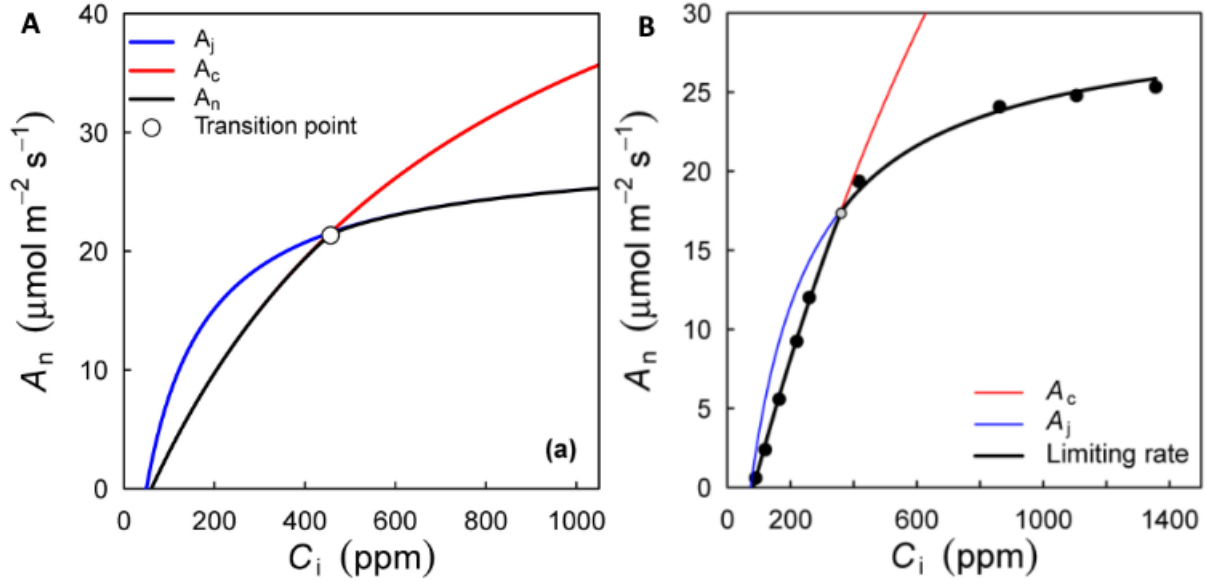


Fig. 8:  $A/C_i$  response curves as modelled with the Farquhar model, using Eq. 1 (a) and Eq. 2 (b). (Duursma, 2015)

### 2.5.2 Photosynthetic parameters

From this fitted model, following parameters can be derived:  $V_{C_{max}}$  is the maximum rate of carboxylation at a given temperature, a measure of how effective the Rubisco enzyme is at fixing  $CO_2$ .  $J_{max}$  is a measure of how fast and effective the electron transport chain and light harvesting systems can regenerate RuBP. These two parameters link back to the abovementioned light dependent and light independent reactions, respectively.  $R_d$  is the mitochondrial respiration in non-photorespiratory processes (Farquhar et al., 1980). These three parameters were calculated using the *Plantecophys* R package (Duursma, 2015).

Additionally, from the fitted curve, three important points can be derived. The first one is the carbon compensation point (**CCP**), at which gross assimilation cancels out respiratory processes and net assimilation rate is zero. Secondly, there is the carbon saturation point (**CSP**), at which 85% of the maximal assimilation rate is attained. Thirdly, the assimilation rate at atmospheric carbon concentrations (**A at  $C_a = 400$  ppm**).

Furthermore, the convexity formula can be slightly altered to derive further parameters:

$$A = \frac{\alpha \cdot C_i + A_{max} - \sqrt{(\alpha \cdot C_i + A_{max})^2 - 4 \cdot \alpha \cdot C_i \cdot A_{max} \cdot \theta}}{2\theta} - R_d \quad (3)$$

where  $\alpha$  is the initial slope of the A/Ci curve, where the concentration of CO<sub>2</sub> is limiting the activity of Rubisco. Ci is intracellular concentration of CO<sub>2</sub>,  $A_{max}$  is the maximal rate of photosynthesis at carbon and light saturating conditions,  $\theta$  (convexity) is the curvature factor of the A/Ci curve (Roberntz & Stockfors, 1998). The convexity parameters were calculated using code by Heberling (2014).

Finally, the relative stomatal limitation ( $L_s$ ) can be estimated by the following equation:

$$L_s = \left(1 - \frac{A_{sat}}{A_{sati}}\right) * 100 \quad (4)$$

where  $A_{sat}$  is the rate of light-saturated photosynthesis at atmospheric carbon concentration and  $A_{sati}$  is the light-saturated photosynthetic rate when intracellular carbon concentration is equal to extracellular (atmospheric) carbon concentration (Sigurdsson et al., 2002).

### 2.5.3 PAR response curves

In irradiance – assimilation (A/I) response curves (Fig. 9), a range of incident PAR intensities is supplied to the leaf. Similar to A/Ci response curves, only one factor changes, in this case PAR, while other factors are kept stable.

A variant of the convexity formula (Eq. 2, Eq. 3) can be used to model the PAR response curves:

$$A = \frac{AQY \cdot I + A_{max} - \sqrt{(AQY \cdot I + A_{max})^2 - 4 \cdot AQY \cdot I \cdot A_{max} \cdot \theta}}{2\theta} - R_{dark} \quad (5)$$

where  $AQY$  is the initial slope or apparent quantum yield, which describes how efficient the leaf is at photosynthesis under PAR limiting conditions. I is the intensity of incident PAR,  $A_{max}$  is the maximal rate of photosynthesis at carbon and PAR saturating conditions,  $\theta$  (convexity) is the curvature factor of the A/I curve and  $R_{dark}$  is the dark respiration (Roberntz & Stockfors, 1998). In order to separate between  $A_{max}$  of A/Ci and A/I response curves, as well as for differentiating between survey and response curves, the distinctions  $A_{max\_Ci}$  and  $A_{max\_I}$  will henceforth be used.

Additionally, from the modelled curve one can derive the light compensation point (**LCP**) and the light saturation point (**LSP**), analogous to the CCP and CSP as mentioned hereinabove.

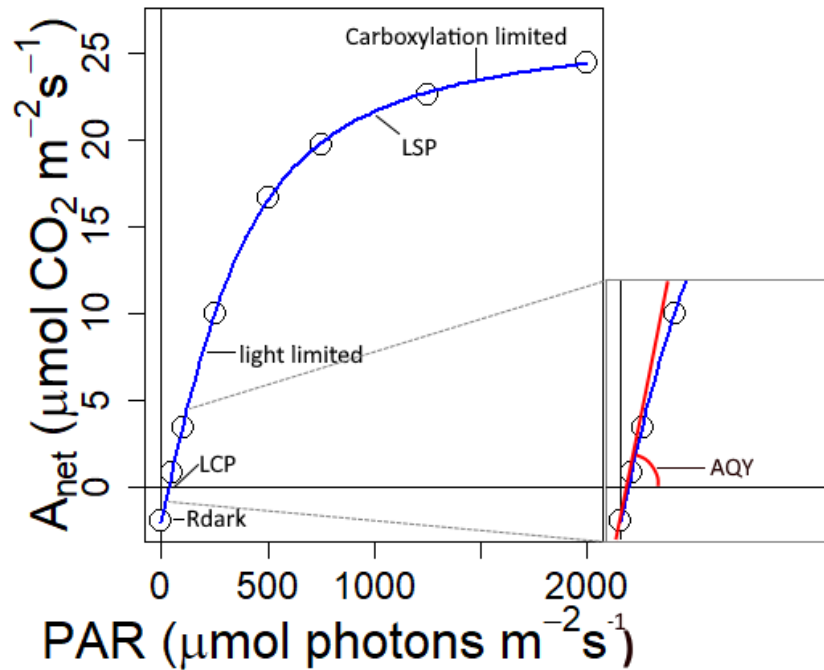


Fig. 9: Example of PAR (A/I) response curve. Following parameters can be identified on the graph:  $R_{dark}$ , intercept with y-axis. LCP, intercept with  $y = 0$ . AQY, initial slope, where light is the limiting factor. LSP, at which 85% of the maximal assimilation rate is attained, where the limiting factor becomes carboxylation rate and efficiency.

## 2.6 Statistical analysis

### 2.6.1 Survey measurements

A two-way ANCOVA model was constructed with site and soil temperature as independent variables (class and continuous, respectively). Six different models were made, with  $A_{net}$ ,  $gsw_{net}$ ,  $A_{sat}$ ,  $gsw_{sat}$ ,  $A_{max}$  and  $gsw_{max}$  as the dependent variables. Each of the models were originally constructed as interactive models. Subsequently, the models were each finetuned by leaving out any non-significant interactions.

In order to check its covariance, the model was then expanded into a three-way ANCOVA model to include leaf N content. In case any of the earlier significant treatment effects disappear, it can be stated these significances were caused by the effect of leaf N content. All models were made in R (4.2.0).

### 2.6.2 Response curves

The response curve parameters were statistically examined using an interactive linear mixed-effect model (using R packages *lme4* and *lmerTest*) with site and soil temperature as independent variables

and plot as random effect, nested in site. Non-significant interactions were subsequently removed. As with the survey measurements, the model was then expanded to investigate the impact of leaf N content as covariable.

In both parts, post hoc analysis was performed using Bartlett's, Shapiro-Wilk and Cook's distance tests to check assumptions of homoscedasticity, normality of residuals and influential outliers, respectively.

## 3. Results

### 3.1 Survey measurements

Net photosynthesis ( $A_{\text{net}}$ ) and stomatal conductance ( $g_{\text{sw}_{\text{net}}}$ ) at ambient  $\text{CO}_2$  and PAR was measured by the initial clamp-on and gives the in-situ carbon assimilation and transpiration fluxes on July 17-18.  $A_{\text{net}}$  was significantly different between sites (Fig. 10), with GO having on average  $20.6 \mu\text{mol m}^{-2} \text{s}^{-1}$  higher assimilation rate than GN with an interactive decrease of  $-1.22 \mu\text{mol m}^{-2} \text{s}^{-1}$  per  $^{\circ}\text{C}$  in GO (Fig. 11c; Table 1). The variation in  $g_{\text{sw}_{\text{net}}}$  was quite high and no significant difference could be detected across treatments or sites (Figs. 10 and 11; Table 1). The N-covariance model showed that these differences between sites were not due to differences in leaf N content (Table 2; Fig. 11).

When light saturated net-photosynthesis ( $A_{\text{sat}}$ ) and stomatal conductance ( $g_{\text{sw}_{\text{sat}}}$ ) at the ambient  $\text{CO}_2$  were compared,  $T_{\text{soil}}$  did not significantly contribute to the model but site did, as did the interaction between the two (Fig. (Figs. 12a and 13c, Table 1).  $A_{\text{sat}}$  showed an increase of  $13.3 \mu\text{mol m}^{-2} \text{s}^{-1}$  in GO in comparison with GN (Fig. 12), with an added decrease of  $-0.79 \mu\text{mol m}^{-2} \text{s}^{-1}$  per  $^{\circ}\text{C}$ . The N-covariance model showed that leaf N content partially explains the variation, but the previous significances (site and site: $T_{\text{soil}}$ ) remain. Additionally, the light-saturated photosynthesis was more reactive to plant differences in N than  $A_{\text{net}}$  was (Table 2, Figs. 11 and 13).  $g_{\text{sw}_{\text{sat}}}$  did not show any significances (Table 1, Figs. 12 and 13).

The light and  $\text{CO}_2$  saturated net-photosynthesis ( $A_{\text{max}}$ ) is indicative of maximal photosynthetic capacity of the *R. acris* plants. This parameter too showed interesting results on July 17-18, as site and interaction  $T_{\text{soil}}$ :site contributed significantly to the model (Table 1).  $A_{\text{max}}$  is  $18.05 \mu\text{mol m}^{-2} \text{s}^{-1}$  higher in GO than in GN with an interactive decrease of  $-0.88 \mu\text{mol m}^{-2} \text{s}^{-1}$  per  $+1^{\circ}\text{C}$  of soil warming (Figs. 14a and 15c). Additionally, leaf N content amounts to a  $+4.9 \mu\text{mol m}^{-2} \text{s}^{-1}$  increase per 1% increase in leaf nitrogen. The parameter  $g_{\text{sw}_{\text{max}}}$  is also reported, but it does not have a physiological meaning when  $\text{CO}_2$  concentrations are saturated and it was not significantly affected by any of the investigated parameters (Table 1; Fig. 14b,d and 15b, d). These findings justified to continue with the gas exchange measurements and make full  $A/C_i$  response curves and light-response curves to dive deeper into the response of photosynthetic machinery to the treatments.

Table 1: Statistical significances of the effects of soil temperature and site, including interaction, on  $A_{net}$ ,  $gsw_{net}$ ,  $A_{sat}$ ,  $gsw_{sat}$ ,  $A_{max}$  and  $gsw_{max}$ . Significances in bold, with different levels of significance indicated with \*\*\* ( $p < 0.001$ ), \*\* ( $p < 0.01$ ), \* ( $p < 0.05$ ) or . ( $p < 0.10$ ).

Significance ( $p < 0.05$ ) in bold indicated with \*, borderline significance ( $0.05 < p < 0.1$ ) in bold indicated with “.”.

	F-statistic	df	Tsoil	Site	Interaction	Tsoil:site	
$A_{net}$	3.24	3, 47	0.88	<b>0.010</b>	**	<b>0.02</b>	*
$gsw_{net}$	1.03	3, 46	0.34	0.92		0.83	
$A_{sat}$	4.84	3, 47	0.96	<b>0.002</b>	**	<b>0.006</b>	**
$gsw_{sat}$	0.87	3, 47	0.55	0.61		0.86	
$A_{max}$	6.85	3, 47	0.24	<b>0.01</b>	*	<b>0.07</b>	.
$gsw_{max}$	0.65	3, 47	0.43	0.67		0.79	

Table 2: Statistical significances of the N-covariance model, including soil temperature, leaf N content and site, including interactions, on  $A_{net}$ ,  $gsw_{net}$ ,  $A_{sat}$ ,  $gsw_{sat}$ ,  $A_{max}$  and  $gsw_{max}$ . Significances in bold, with different levels of significance indicated with \*\*\* ( $p < 0.001$ ), \*\* ( $p < 0.01$ ), \* ( $p < 0.05$ ) or . ( $p < 0.10$ ).

	F-statistic	df	Tsoil	N%	site	Tsoil:N%	Tsoil:site	N%:site					
$A_{net}$	2.47	4, 46	0.87	0.82	<b>0.01</b>	*	0.35	<b>0.02</b>	*	0.53			
$gsw_{net}$	1.09	3, 46	0.33	0.63	0.26		0.25	0.91		0.50			
$A_{sat}$	4.05	5, 45	<b>0.08</b>	.	<b>0.04</b>	*	<b>0.02</b>	*	<b>0.08</b>	.	<b>0.02</b>	*	0.80
$gsw_{sat}$	0.87	3, 47	0.47	0.97	0.29		0.24	0.83		0.44			
$A_{max}$	7.01	3, 47	<b>0.05</b>	.	<b>0.06</b>	.	<b>0.05</b>	*	0.83	0.19	0.56		
$gsw_{max}$	0.65	3, 47	0.32	0.78	0.54		0.22	0.74		0.48			

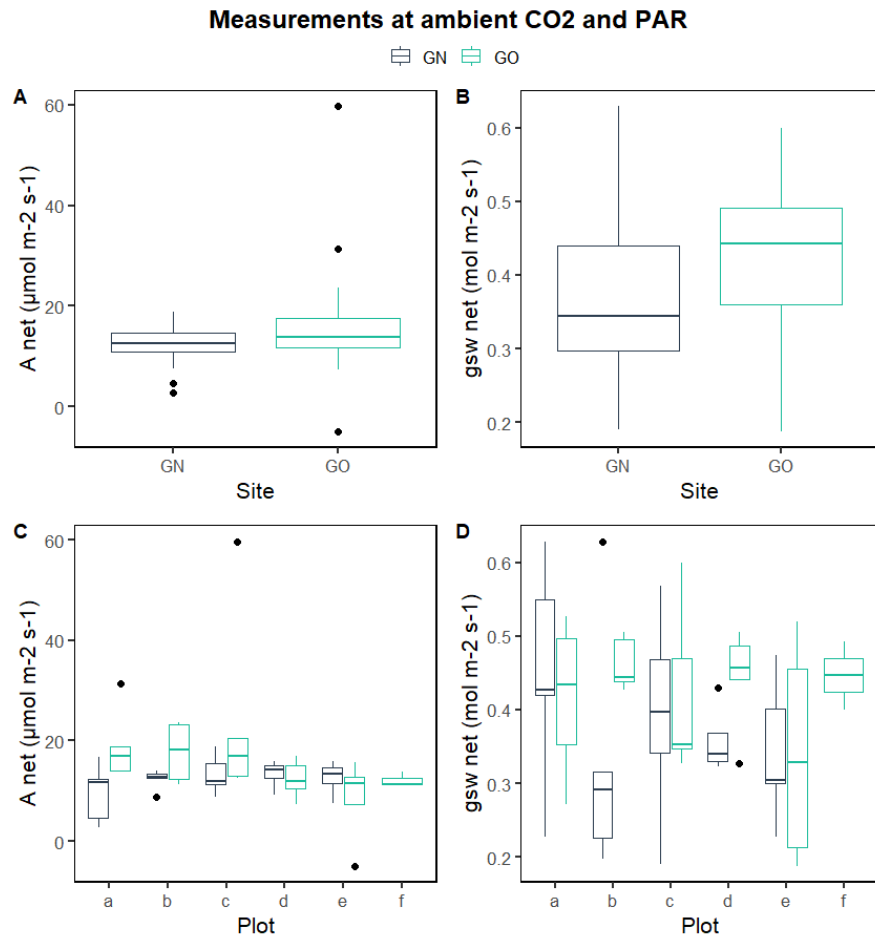


Fig. 10: Assimilation rate (left) and  $gsw$  (right) of survey measurements at ambient CO<sub>2</sub> and PAR, plotted per site (top) and plot (bottom).

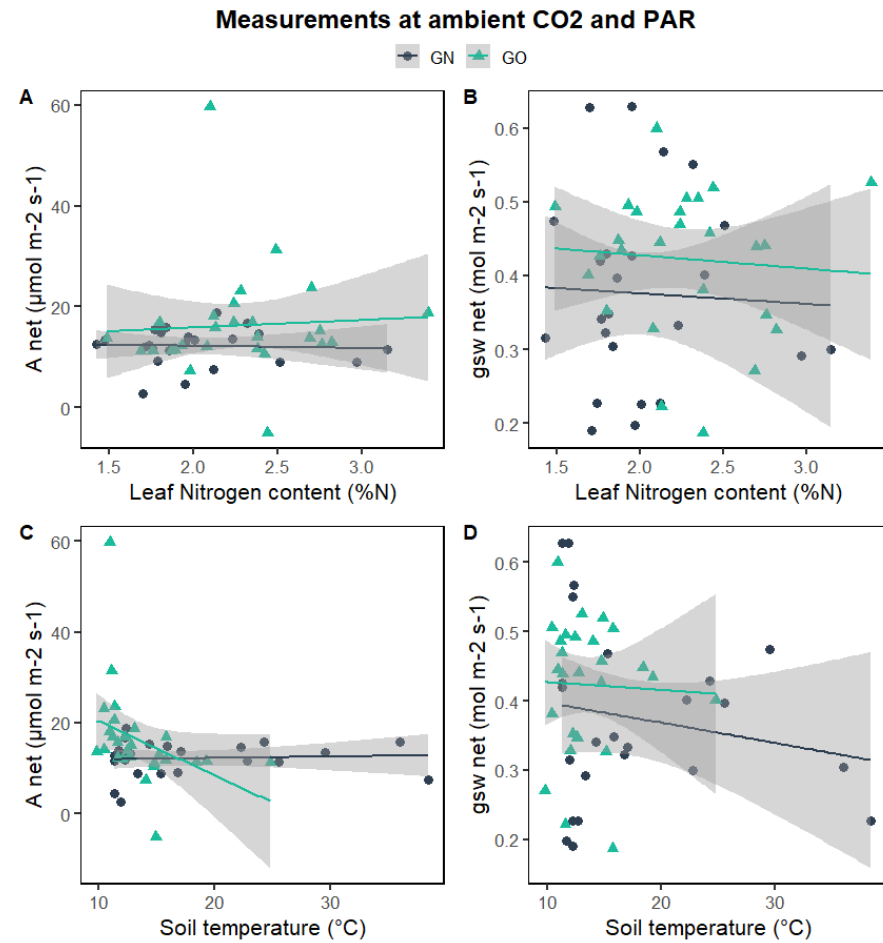


Fig. 11: Assimilation rate (left) and  $gsw$  (right) of survey measurements at ambient CO<sub>2</sub> and PAR, plotted per leaf N content (top) and soil temperature (bottom).

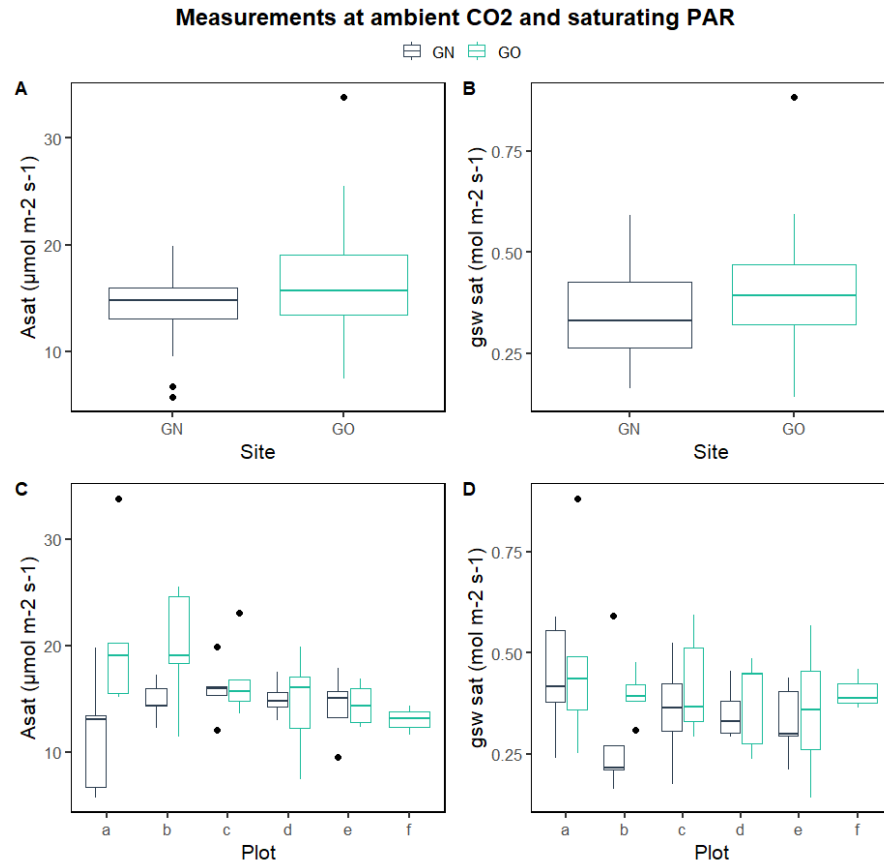


Fig. 12:  $A_{\text{sat}}$  (left) and  $g_{\text{sw}}$  (right) of survey measurements at ambient CO<sub>2</sub> and saturating PAR, plotted per site (top) and plot (bottom).

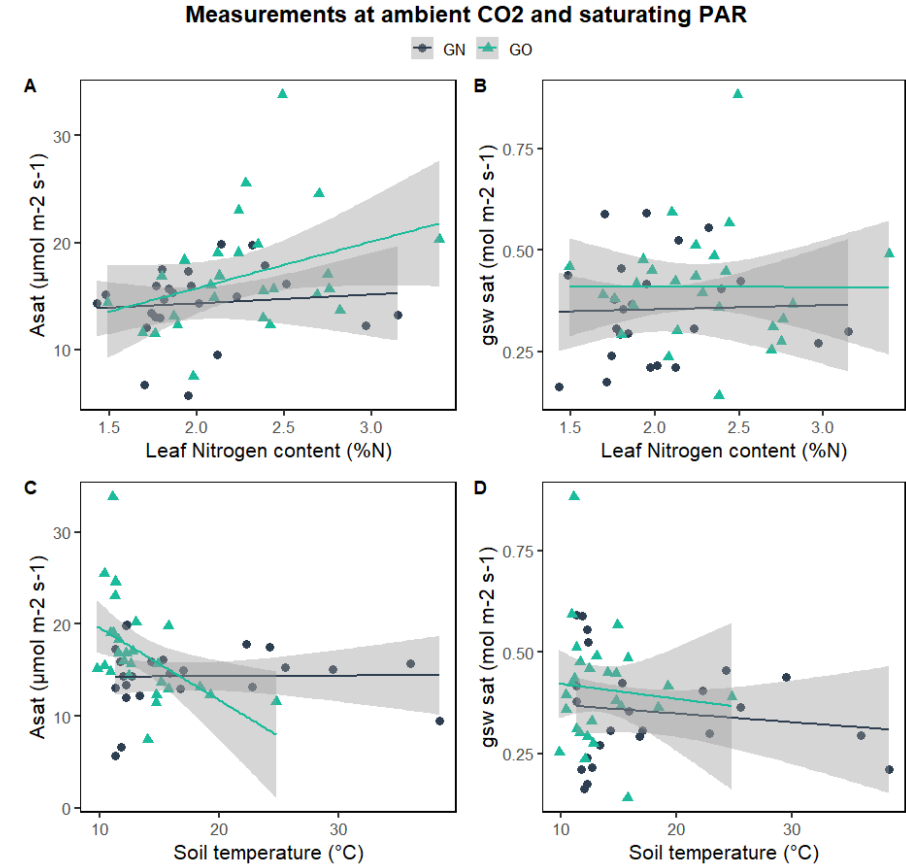


Fig. 13: Assimilation rate (left) and  $g_{\text{sw}}$  (right) of survey measurements at ambient CO<sub>2</sub> and saturating PAR, plotted per leaf N content (top) and soil temperature (bottom).

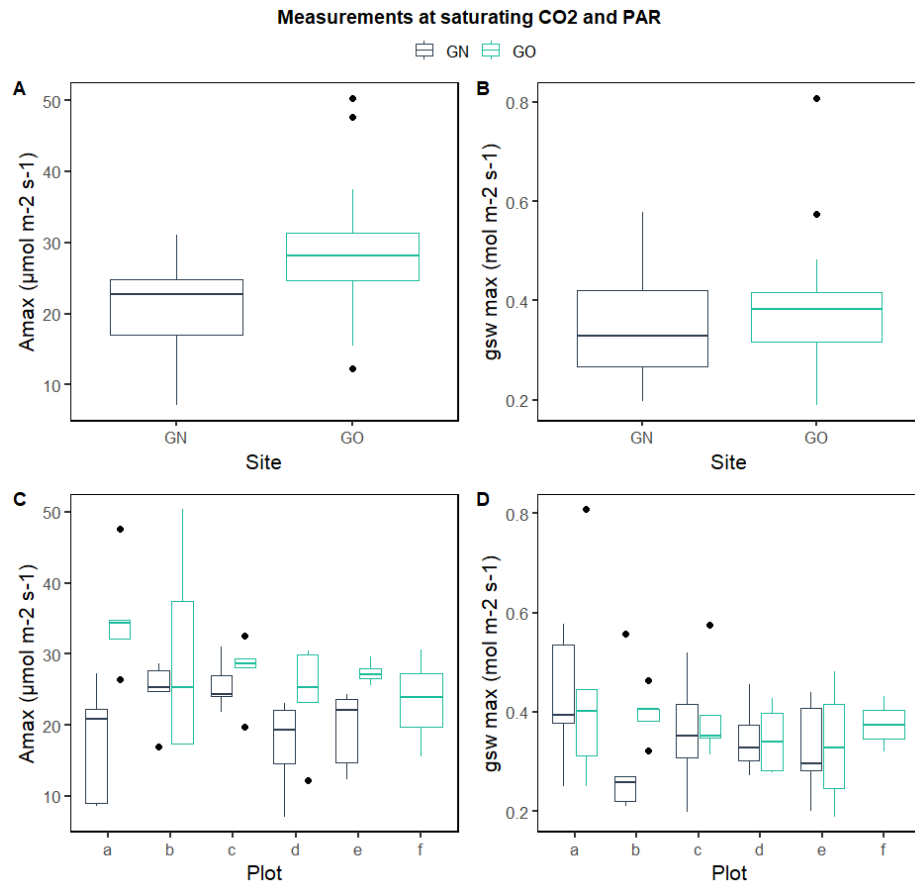


Fig. 14: Assimilation rate (left) and gsw (right) of survey measurements at saturating CO<sub>2</sub> and PAR, plotted per site (top) and plot (bottom).

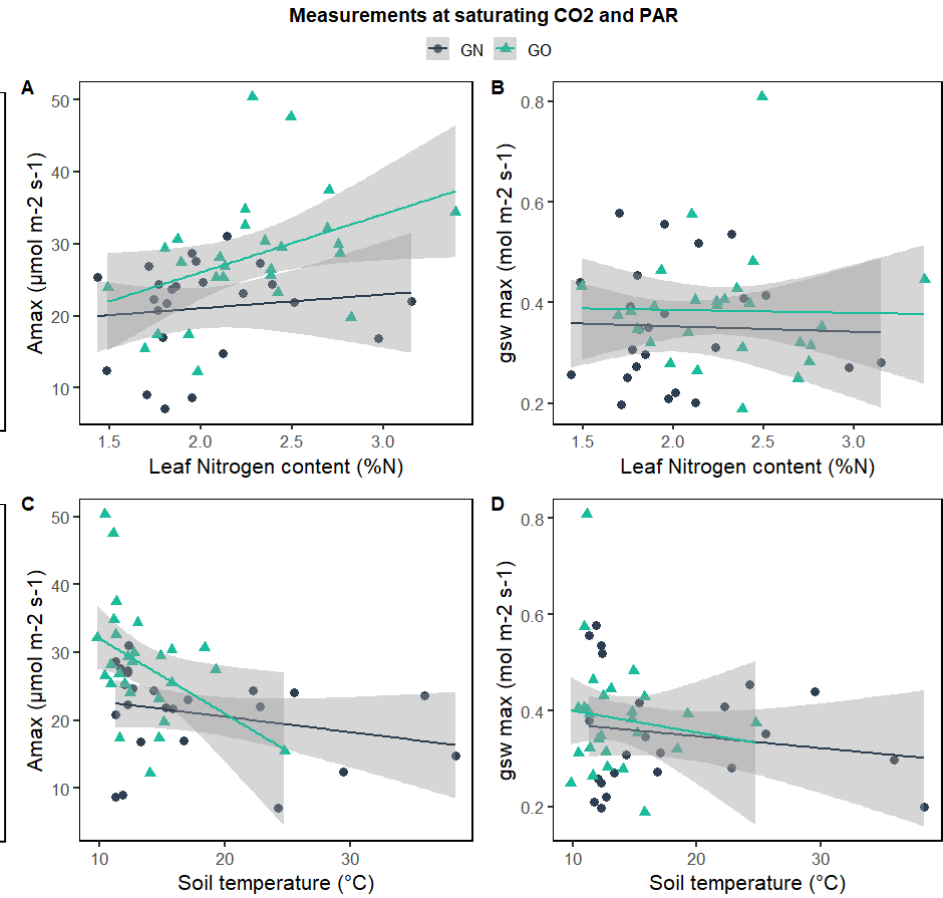


Fig. 15: Assimilation rate (left) and gsw (right) of survey measurements at saturating CO<sub>2</sub> and PAR, plotted per leaf N content (top) and soil temperature (bottom).

## 3.2 Photosynthesis response curves

To study the photosynthetic system in more depth, a total of 54 A/Ci and A/I response curves were taken – 12 in GNa and GNe, 15 in GOa and GOe (boxplot summaries in Addendum 2, Fig. 26). The individual curves were fitted with the Farquhar and convexity formulas described in Methods and the Farquhar and convexity parameters were derived (Table 3). The average A/Ci and A/I response curves are shown in Fig. 16 and Fig. 17 and the statistical difference between treatments in Table 4, statistical analysis of N-covariance model in Table 5. Statistically different parameters are shown in Figs. 18, 19, 20 and 21.

### 3.2.1 A/Ci convexity parameters

First, the parameters derived from the fitted A/Ci convexity formula (Eq. 3):  $A_{\max\_Ci}$ ,  $\alpha$ ,  $R_d$  and  $\theta$ . The first parameter,  $A_{\max\_Ci}$ , is the same parameter as the one looked at with the survey measurements (light- and CO<sub>2</sub>-saturated net-photosynthesis); now with more replicates, but only comparing two soil temperature warming levels (a and e). The earlier results were only partly replicated. Now  $A_{\max\_Ci}$  was not significantly affected by Tsoil or site, but only by N% (Tables 4 and 5). Alpha (carboxylation efficiency) and  $R_d$  differed significantly between sites: alpha started off 0.0505 higher in GO than in GN, with a decrease of -0.003 per °C of soil warming in GO;  $R_d$  was 1.8  $\mu\text{mol s}^{-1} \text{m}^{-2}$  higher in GO relative to GN, with a decrease of -0.1  $\mu\text{mol s}^{-1} \text{m}^{-2}$  per °C. However, the N-covariance model showed that this effect between sites was mostly explained by highly significant impact of leaf N content: all three parameters were positively related to leaf N%, which is shown for  $A_{\max\_Ci}$ ,  $\alpha$  in Fig. 20.  $A_{\max\_Ci}$  increased by 11.5  $\mu\text{mol s}^{-1} \text{m}^{-2}$  and alpha increased by 0.032 by 1% increase in leaf N. Further, in a follow-up analysis leaf N% was not shown to be significantly affected by neither Tsoil nor site (Tables 6 and 7), so it is representing and independent environmental driver in the field experiments.

The two additional points derived from the A/Ci curves, the carbon compensation point (CCP) and the carbon saturation point (CSP) were not significantly affected by Tsoil, site nor N%. However, the third parameter (A at Ca = 400 ppm) was affected, with a difference of +11.4  $\mu\text{mol s}^{-1} \text{m}^{-2}$  in GO relative to GN with an interactive negative effect of -0.6  $\mu\text{mol s}^{-1} \text{m}^{-2}$  per °C of soil warming in GO. This parameter in the A/Ci curve is comparable to  $A_{\text{sat}}$  from the survey measurements. As was found for  $A_{\text{sat}}$ , this parameter was significantly and positively related to both site and N% (Tables 4 and 5, Figs. 18e and 19d).

The only significant Tsoil effect observed in the A/Ci response curve N-covariance analysis was the apparent negative influence on intercellular CO<sub>2</sub> concentration at Ca = 400 ppm (-0.68 ppm Ci per °C

Tsoil; Table 5, Fig 20) a response only driven by GN and through N-covariance, but as neither net photosynthesis nor  $L_s$  were significantly affected by this small change in  $C_i$ , this finding is of limited interest.

### 3.2.2 A/ $C_i$ Farquhar parameters

Moving on to the results of the Farquhar model on the limiting factors for maximum photosynthetic capacity, the modelling is shown in Fig. 16. Both  $V_{C_{max}}$  and  $J_{max}$  were significantly affected by site and site:Tsoil interaction.  $V_{C_{max}}$  showed a difference of  $+51 \mu\text{mol s}^{-1} \text{m}^{-2}$  in GO compared to GN, with a decrease of  $-2.7 \mu\text{mol s}^{-1} \text{m}^{-2}$  per  $^{\circ}\text{C}$  of soil warming and  $J_{max}$  showed similar differences:  $84.7 \mu\text{mol s}^{-1} \text{m}^{-2}$  in higher in GO than GN, with an interactive decrease of  $-4.3 \mu\text{mol s}^{-1} \text{m}^{-2}$  per  $^{\circ}\text{C}$  of soil warming (Fig. 18a-b) The N-covariance analysis, however, showed that differences in both parameters were mainly caused by variation in N% (Table 5, Fig. 20a-b).

### 3.2.3 A/I convexity parameters

However, plants rarely operate at their maximum capacity for long in nature and therefore the A-I curves may be of more interest (Tables 3, 4 and 5). It should be noted that during the measurements the leaves were kept at saturated  $\text{CO}_2$  concentrations during the A-I measurements, which allows for looking at the photosynthetic reactions without confounding effects of potentially different gsws.

First, let's look at the four convexity parameters of the A-I response curves that are shown in Fig. 17:  $A_{max\_I}$ , AQY,  $R_{dark}$  and  $\theta$ .  $A_{max\_I}$  (here measured at saturating  $\text{CO}_2$ ) shows the same N-sensitivity as  $A_{max\_C_i}$ . It increased by  $16.3 \mu\text{mol s}^{-1} \text{m}^{-2}$  for each 1% increase in leaf N (Fig. 19a). However, whereas  $A_{max\_C_i}$  did not show significant difference between sites,  $A_{max\_I}$  does:  $+13.0 \mu\text{mol s}^{-1} \text{m}^{-2}$  higher in GO than in GN, with an additional effect in GO of  $-1.2 \mu\text{mol s}^{-1} \text{m}^{-2}$  per  $^{\circ}\text{C}$ . However, the N-covariance model showed that most of this difference lies in leaf N content. On the other hand, dark respiration ( $R_{dark}$ ) was not significantly affected by any of the explaining parameters and convexity ( $\theta$ ) of the A-I response curve only showed significances in the N-covariance model (Tsoil ( $-0.007$  per  $1^{\circ}\text{C}$  warming), N% and interaction between those). AQY, too, was only significantly different between sites in the N-covariance model (on average  $0.013$  higher in GO than GN; Table 3, Table 5, Fig. 18d).

The LCP of the A-I curves (at which PAR net photosynthesis becomes positive) showed no significance in the first model, only showing a near significant changes to Tsoil in the N-covariance model (only  $-3.7 \mu\text{mol s}^{-1} \text{m}^{-2}$  PAR per  $^{\circ}\text{C}$  of warming, mostly driven by GO; Fig 20) and N content ( $+537 \mu\text{mol s}^{-1} \text{m}^{-2}$  PAR per percent additional nitrogen (Fig 21); but as the interaction between those two drivers (Tsoil and N%) was not significant (Table 5) it was not easy to interpret these apparent changes in LCP or

estimate their impact on carbon uptake. The final derived parameter of the A-I curves, the light saturation point (LSP) showed large differences between sites, starting off at +1562  $\mu\text{mol s}^{-1} \text{m}^{-2}$  in GO compared to GN, but with a steep decrease of -95  $\mu\text{mol s}^{-1} \text{m}^{-2}$  per  $^{\circ}\text{C}$  soil warming in GO. This significance remained in the N-covariance model, additionally showing that LSP was significantly affected by N% (Table 4; Table 5).

Table 3: Treatment averages ( $\pm$  SE) of Farquhar parameters of A/Ci response curves –  $V_{C_{\max}}$ ,  $J_{\max}$  &  $R_d$  –, convexity parameters of A/Ci response curves –  $A_{\max_{\text{Ci}}}$ ,  $\alpha$ ,  $R_d$ ,  $\theta$ , Carbon compensation point (CCP), CSP (Carbon saturation point) and A at  $\text{Ca} = 400$  ppm –, convexity parameters of A/I response curves –  $A_{\max_{\text{I}}}$ , apparent quantum yield (AQY),  $R_{\text{dark}}$ ,  $\theta$ , light compensation point (LCP) & light saturation point (LSP).

Treatment	GNa	$\pm$ SE	GNe	$\pm$ SE	GOa	$\pm$ SE	GOe	$\pm$ SE
$V_{C_{\max}}$ ( $\mu\text{mol s}^{-1} \text{m}^{-2}$ )	73	4	70	4	85	5	75	7
$J_{\max}$ ( $\mu\text{mol s}^{-1} \text{m}^{-2}$ )	138	8	132	9	163	10	146	12
$R_d$	0.78	0.16	0.83	0.13	0.71	0.14	0.69	0.14
$A_{\max_{\text{Ci}}}$ ( $\mu\text{mol s}^{-1} \text{m}^{-2}$ )	28.6	1.3	27.4	1.7	33.1	2.0	29.6	2.0
$\alpha$	0.06	0.00	0.06	0.00	0.08	0.00	0.07	0.01
$R_d$	2.64	0.21	2.77	0.18	3.08	0.15	2.71	0.22
$\theta$	0.96	0.01	0.97	0.01	0.97	0.01	0.96	0.01
CCP (ppm)	40.7	2.1	43.4	1.2	40.8	1.7	40.8	2.3
CSP (ppm)	474	30	453	21	450	18	485	26
Ci at $\text{Ca} = 400$ ppm (ppm)	323	3	316	5	331	4	325	5
A at $\text{Ca} = 400$ ppm ( $\mu\text{mol s}^{-1} \text{m}^{-2}$ )	16.8	0.8	16.2	0.8	20.3	1.3	17.6	1.4
A at Ci = 400 ppm ( $\mu\text{mol s}^{-1} \text{m}^{-2}$ )	18.8	1.3	17.8	1.2	22.2	1.5	19.0	1.7
Ls (%)	10.1	2.2	11.9	1.8	7.8	1.8	7	4
$A_{\max_{\text{I}}}$ ( $\mu\text{mol s}^{-1} \text{m}^{-2}$ )	28.8	1.4	29.4	2.7	34.1	2.3	30.8	2.6
AQY	0.058	0.004	0.057	0.004	0.071	0.006	0.068	0.003
$R_{\text{dark}}$	2.0	0.5	1.61	0.15	1.8	0.3	1.76	0.23
$\theta$	0.71	0.03	0.56	0.13	0.68	0.03	0.66	0.03
LCP ( $\mu\text{mol s}^{-1} \text{m}^{-2}$ )	36	8	30	4	27	4	27	4
LSP ( $\mu\text{mol s}^{-1} \text{m}^{-2}$ )	1260	120	2133	900	1386	210	1259	170

Table 4: Statistical analysis of original model, excluding N covariance: Farquhar parameters of A/Ci response curves –  $V_{C_{max}}$ ,  $J_{max}$  and  $R_d$  –, convexity parameters of A/Ci response curves –  $A_{max\_Ci}$ ,  $\alpha$ ,  $R_d$ ,  $\theta$ , Carbon compensation point (CCP), CSP (Carbon saturation point) and A at  $C_a = 400$  ppm –, convexity parameters of A/I response curves –  $A_{max\_I}$ , apparent quantum yield (AQY),  $R_{dark}$ ,  $\theta$ , light compensation point (LCP) and light saturation point (LSP). Significances in bold, with different levels of significance indicated with \*\*\* ( $p < 0.001$ ), \*\* ( $p < 0.01$ ), \* ( $p < 0.05$ ) or . ( $p < 0.10$ ).

Parameter	Tsoil p-value	Site p-value	Interaction p-value
$V_{C_{max}}$	0.75	<b>0.02</b> *	<b>0.03</b> *
$J_{max}$	0.74	<b>0.04</b> *	<b>0.07</b> .
$R_d$	0.74	0.66	0.96
$A_{max\_Ci}$	0.73	0.35	0.11
A	0.98	<b>0.02</b> *	<b>0.03</b> *
$R_d$	0.54	<b>0.07</b> .	<b>0.09</b> .
$\theta$	0.50	0.89	0.80
CCP	0.34	0.86	0.84
CSP	0.60	0.27	0.25
Ci at $C_a = 400$ ppm	0.31	0.33	0.28
A at $C_a = 400$ ppm	0.74	<b>0.02</b> *	<b>0.03</b> *
A at Ci = 400 ppm	0.75	<b>0.03</b> *	<b>0.05</b> *
Ls	0.57	0.75	0.52
$A_{max\_I}$	0.98	<b>0.07</b> .	<b>0.09</b> .
AQY	0.99	0.89	0.56
$R_{dark}$	0.43	0.86	0.74
$\theta$	0.26	0.35	0.34
LCP	0.36	0.75	0.57
LSP	0.71	<b>0.01</b> *	<b>0.01</b> *

Table 5: Statistical analysis of model including N covariance: Farquhar parameters of A/Ci response curves –  $V_{c_{max}}$ ,  $J_{max}$  &  $R_d$  –, convexity parameters of A/Ci response curves –  $A_{max_{Ci}}$ ,  $\alpha$ ,  $R_d$ ,  $\theta$ , Carbon compensation point (CCP), CSP (Carbon saturation point) & A at  $Ca = 400$  ppm –, convexity parameters of A/I response curves –  $A_{max_I}$ , apparent quantum yield (AQY),  $R_{dark}$ ,  $\theta$ , light compensation point (LCP) and light saturation point (LSP). Obtained from the nitrogen covariance model. Significances in bold, with different levels of significance indicated with \*\*\* ( $p < 0.001$ ), \*\* ( $p < 0.01$ ), \* ( $p < 0.05$ ) or . ( $p < 0.10$ ).

Parameter	Tsoil p-value		N% p-value		Site p-value		Significant interaction?	
$V_{c_{max}}$	0.62		<b>&lt;0.001</b>	***	0.27			
$J_{max}$	0.50		<b>&lt;0.001</b>	***	0.16			
$R_d$	0.37		0.28		0.69			
$A_{max_{Ci}}$	0.41		<b>&lt;0.001</b>	***	0.19			
A	0.63		<b>&lt;0.001</b>	***	0.15			
$R_d$	0.64		<b>&lt;0.001</b>	***	0.39			
$\theta$	0.28		0.53		0.66			
CCP	0.36		0.42		0.95			
CSP	0.44		0.65		0.97			
Ci at $Ca = 400$ ppm	<b>0.01</b>	*	<b>&lt;0.01</b>	**	0.27			
A at $Ca = 400$ ppm	0.38		<b>&lt;0.001</b>	***	<b>0.08</b>	.		
A at Ci = 400 ppm	0.56		<b>&lt;0.001</b>	***	0.28			
Ls	0.20		0.64		0.30			
$A_{max_I}$	0.93		<b>&lt;0.001</b>	***	0.25			
AQY	0.37		0.4		<b>0.01</b>	**		
$R_{dark}$	0.40		0.98		0.67			
$\theta$	<b>0.01</b>	**	<b>0.078</b>	.	0.66		<b>Tsoil : N% (p = 0.002)</b>	**
LCP	<b>0.06</b>	.	<b>0.0962</b>	.	0.12		<b>Tsoil : N% (p = 0.08)</b>	.
LSP	0.99		<b>0.05</b>	*	<b>0.07</b>	.	<b>Tsoil : site (p = 0.05)</b>	*

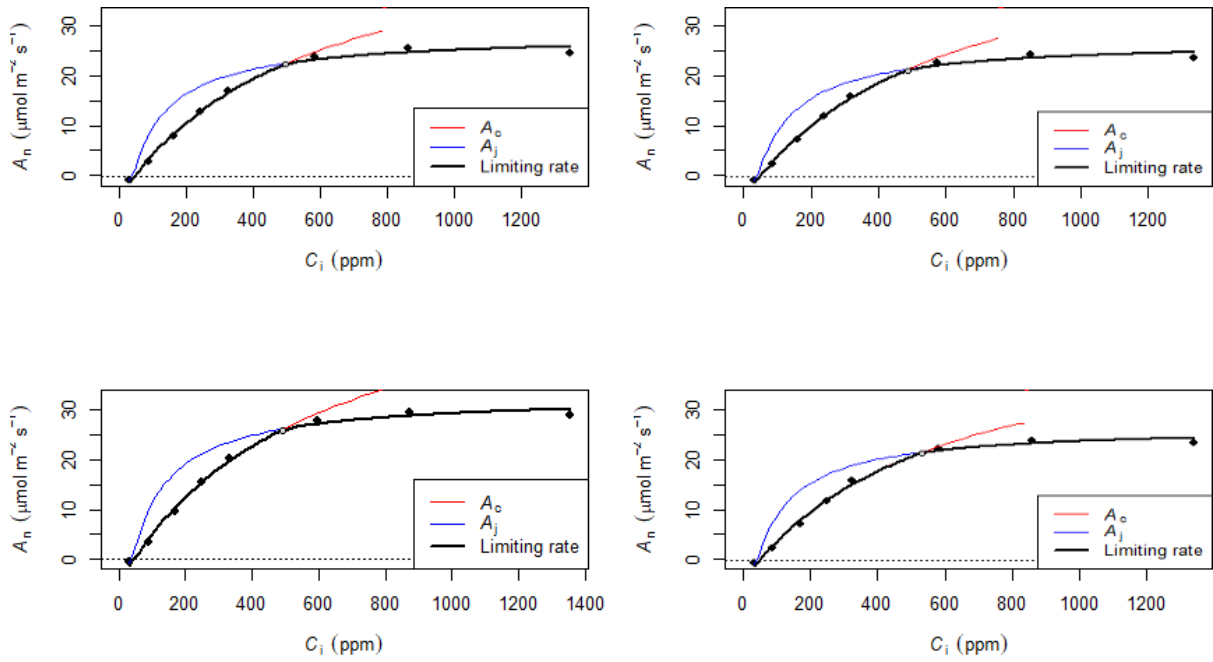


Fig. 16: Fitted  $A/C_i$  curves of the averages of GNa (a), GNe (b), GOa (c) and GOe (d).

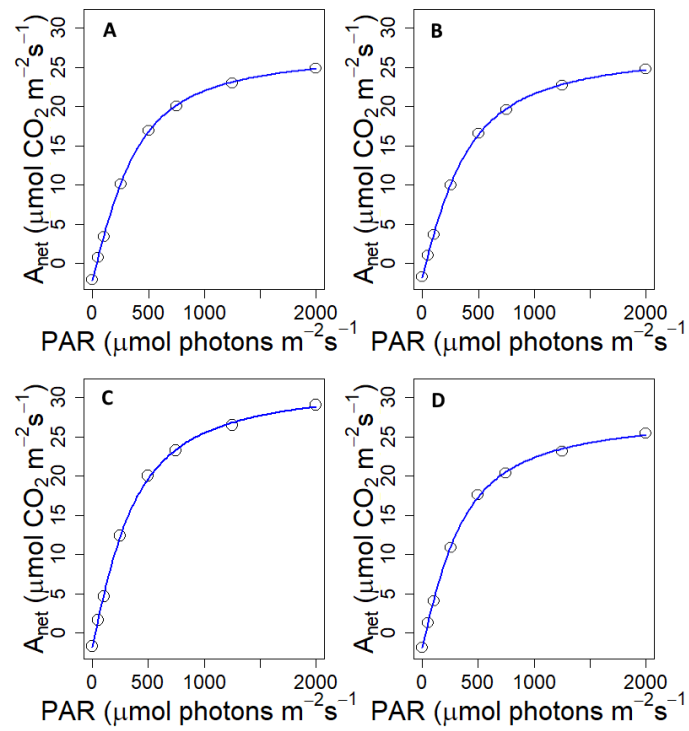


Fig. 17: Fitted  $A/I$  convexity curves of the averages of GNa (a), GNe (b), GOa (c) and GOe (d).

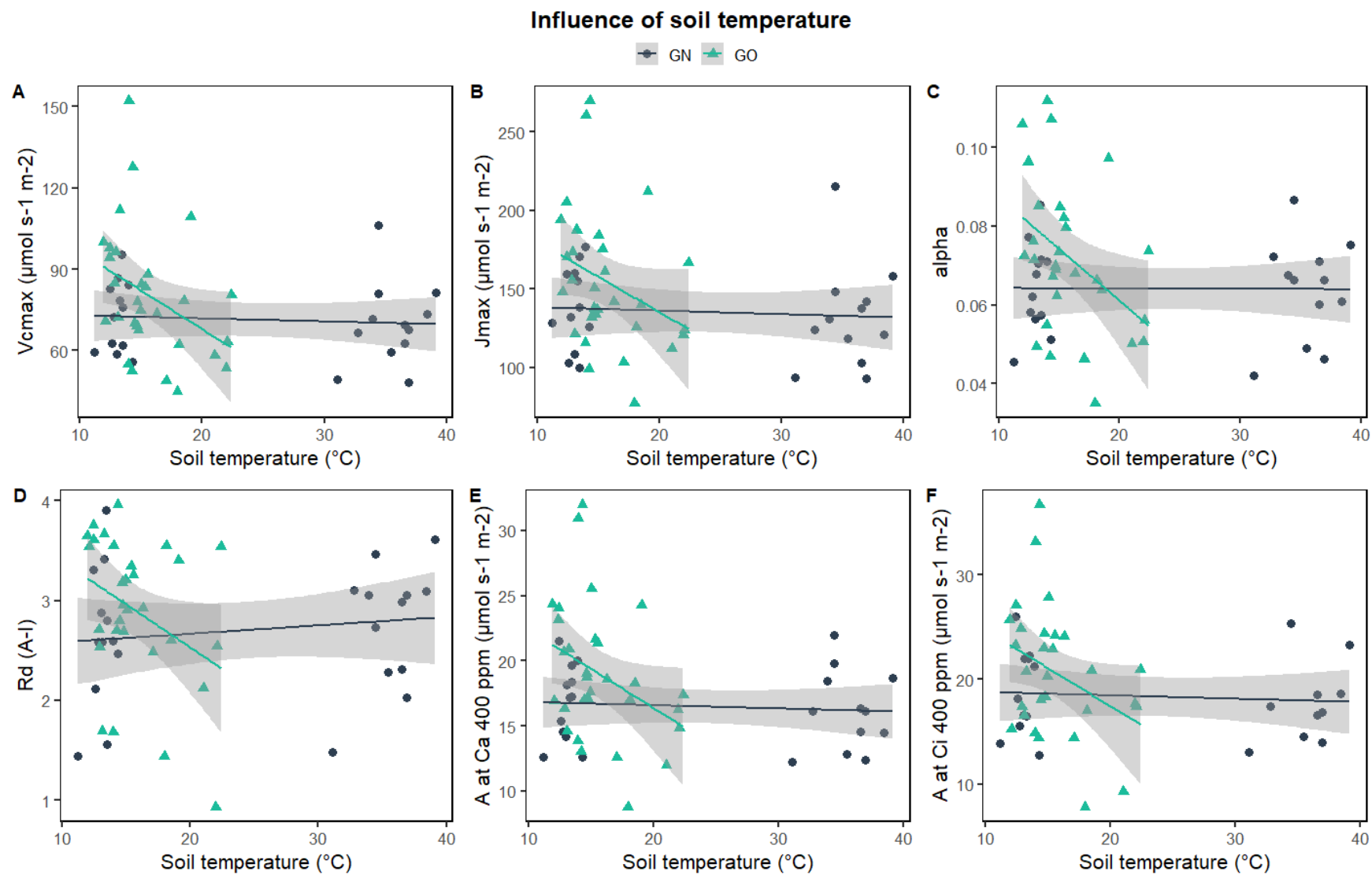


Fig. 18: Influence of soil temperature on a)  $V_{cmax}$ , b)  $J_{max}$ , c)  $\alpha$ , d)  $R_d$  of light response, e)  $A$  at  $C_a = 400$  ppm and f)  $A$  at  $C_i = 400$  ppm.

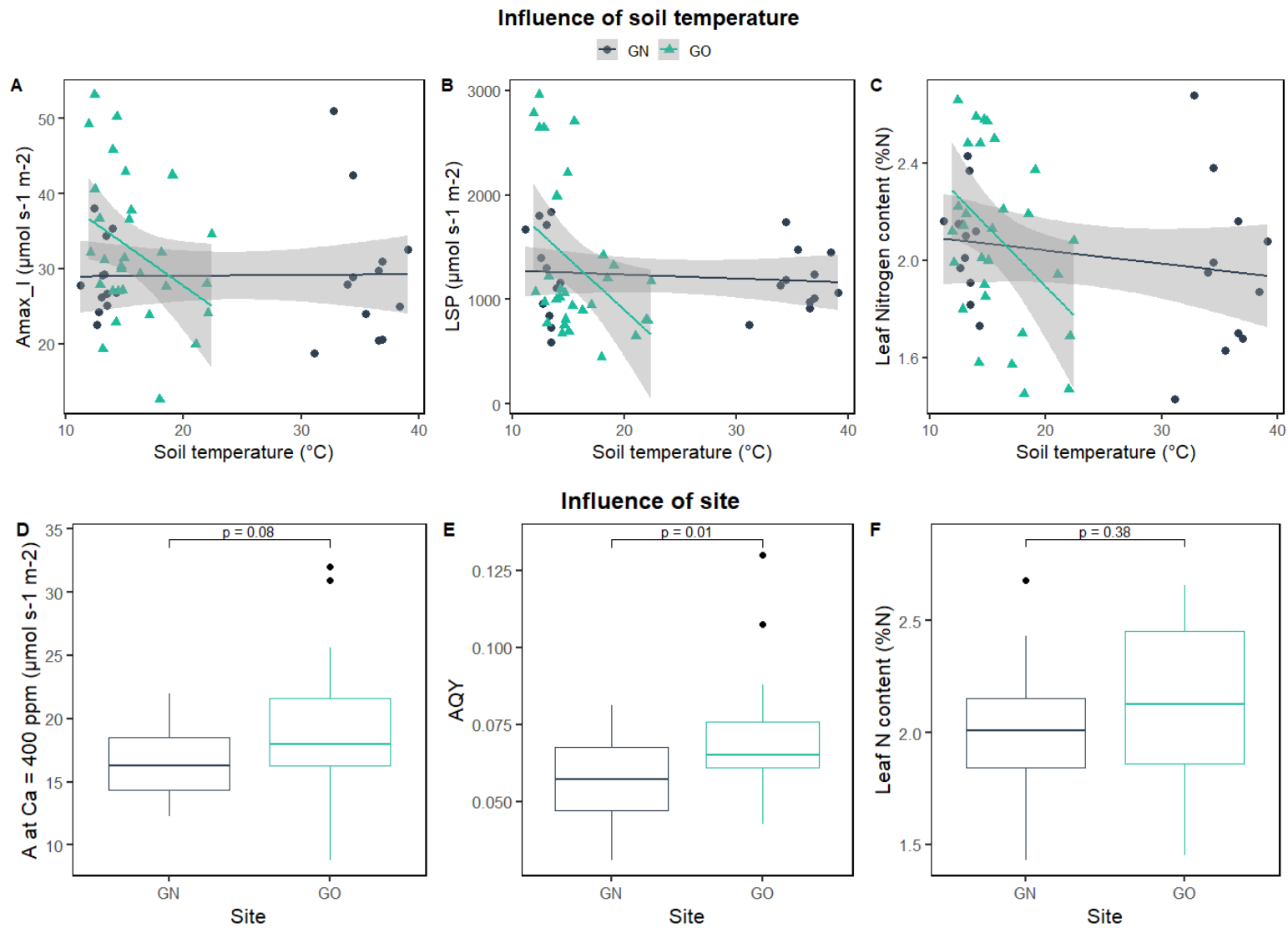


Fig. 19: Influence of soil temperature on a)  $A_{max\_l}$ , b) LSP and c) leaf N content. Influence of site on d) A at Ca = 400 ppm and e) AQY and f) leaf N content.

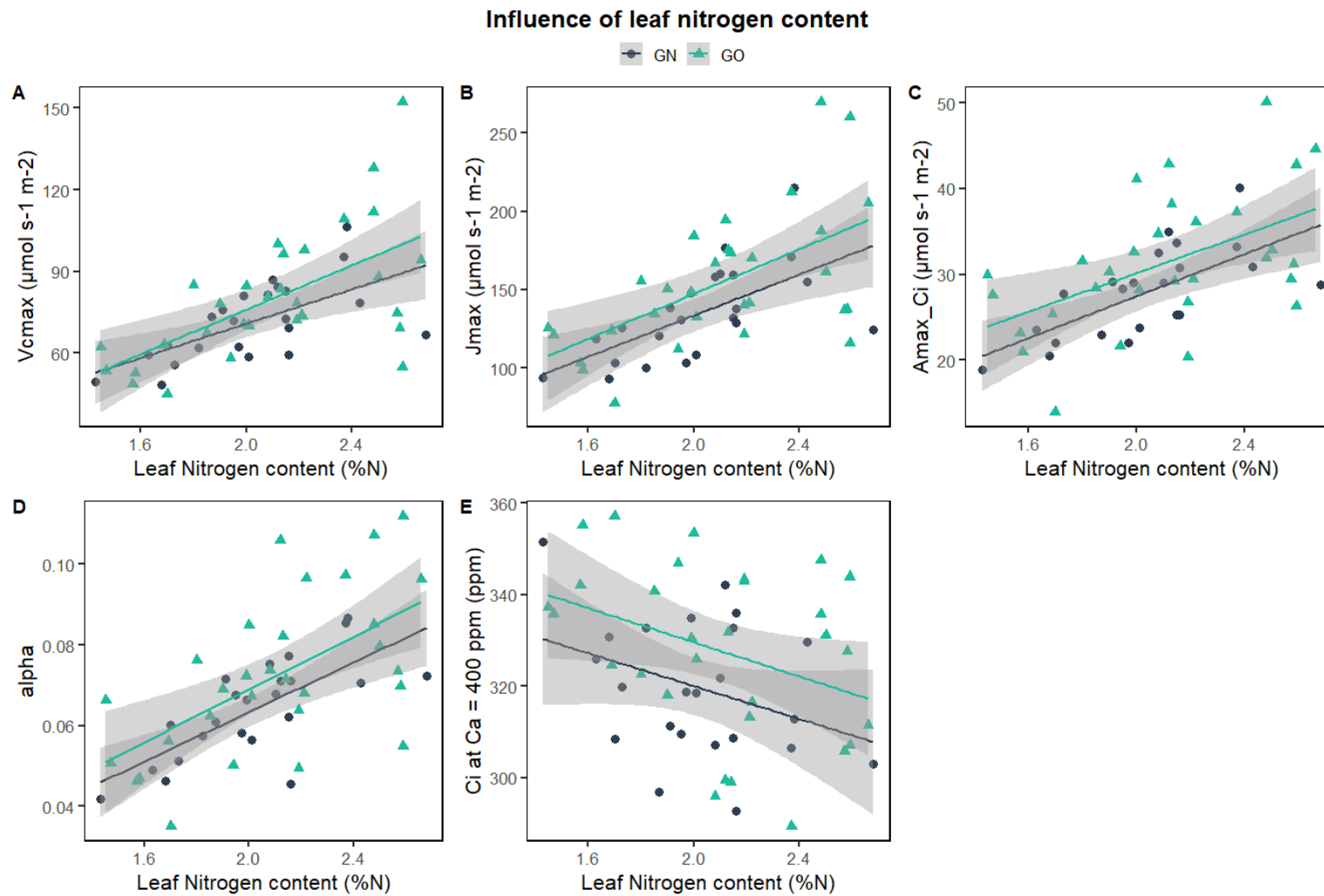


Fig. 20: Influence of leaf N content on a)  $V_{cmax}$ , b)  $J_{max}$ , c)  $A_{max\_Ci}$ , d)  $\alpha$ , e)  $C_i$  at  $C_a = 400$  ppm.

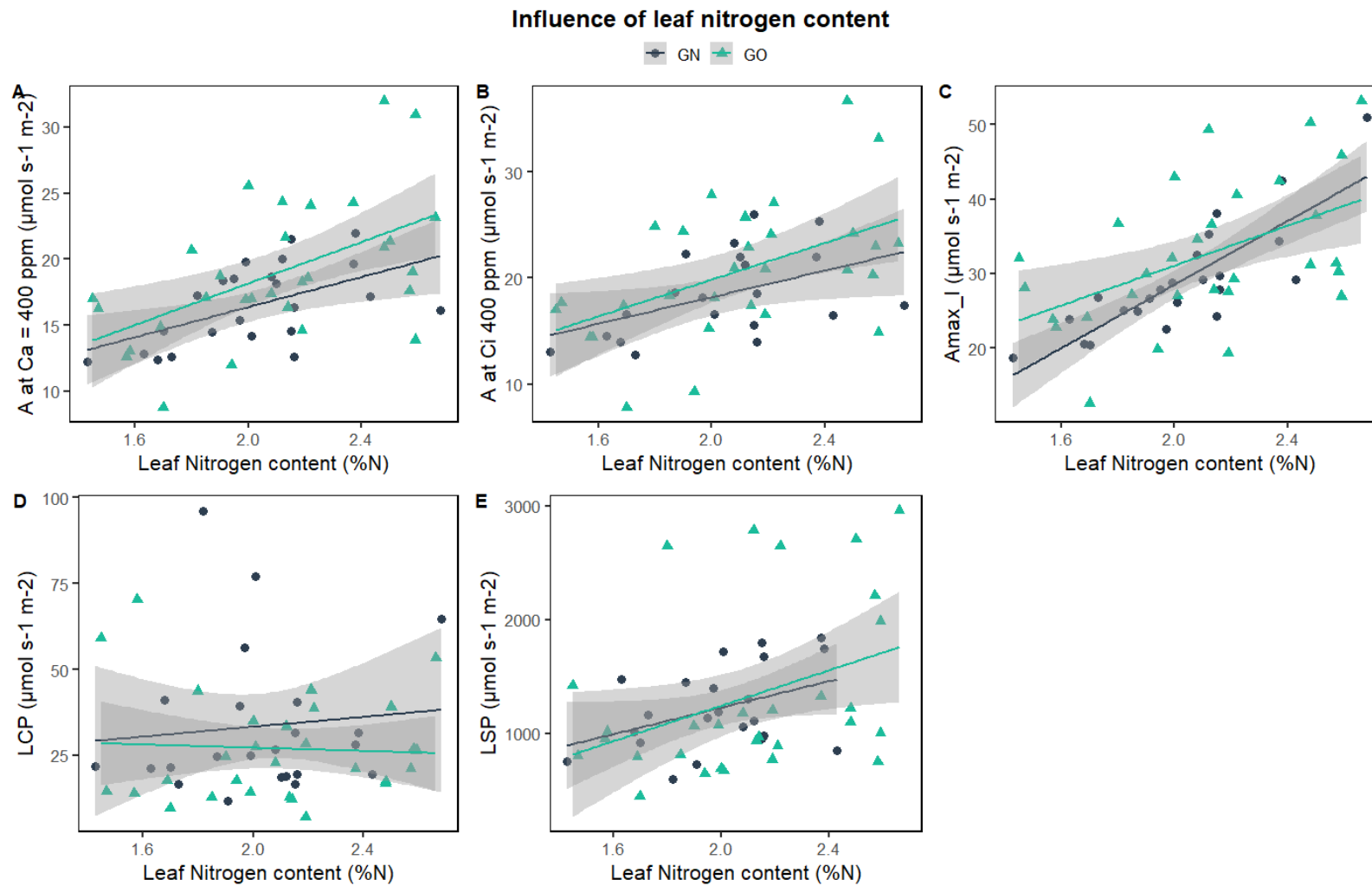


Fig. 21: Influence of leaf N content on a) A at Ca = 400 ppm, b) A at Ci = 400 ppm, c)  $A_{\text{max}_l}$ , d) LCP, e) LSP.

### 3.3 C/N, stable isotopes and SLA

Table 6: Treatment averages ( $\pm$  SE) of carbon (C) and nitrogen (N) concentrations and stable isotope delta values, and of specific leaf area (SLA).

Parameter	GNa	$\pm$ SE	GNe	$\pm$ SE	GOa	$\pm$ SE	GOe	$\pm$ SE
Leaf C content (%)	41.80	0.16	41.38	0.27	40.97	0.19	41.34	0.33
$\delta^{13}\text{C}$ (‰ V-PDB)	-29.32	0.24	-29.10	0.20	-29.88	0.21	-29.56	0.25
Leaf N content (%)	2.08	0.06	1.96	0.11	2.14	0.07	2.07	0.11
$\delta^{15}\text{N}$ (‰ air $\text{N}_2$ )	-3.34	0.26	-2.43	0.34	-4.64	0.36	-1.90	0.50
SLA ( $\text{cm}^2 \text{g}^{-1}$ )	180.32	13.59	164.98	6.20	172.50	10.85	173.52	9.02

Table 7: Statistical analysis of the original model, excluding N covariance: the effects of carbon (C) and nitrogen (N) concentrations and stable isotope delta values, and of specific leaf area (SLA). Significances in bold, with different levels of significance indicated with \*\*\* ( $p < 0.001$ ), \*\* ( $p < 0.01$ ), \* ( $p < 0.05$ ) or . ( $p < 0.10$ ).

Parameter	Tsoil p-value	Site p-value	Interaction p-value
Leaf C content	0.30	0.40	0.44
$\delta^{13}\text{C}$	0.23	0.22	0.14
Leaf N content	0.63	0.20	0.29
$\delta^{15}\text{N}$	0.61	0.13	0.11
Specific leaf area	0.73	0.58	0.32

Table 8: Statistical analysis of the model including N covariance: the effects of carbon (C) and nitrogen (N) concentrations and stable isotope delta values, and of specific leaf area (SLA). Significances in bold, with different levels of significance indicated with \*\*\* ( $p < 0.001$ ), \*\* ( $p < 0.01$ ), \* ( $p < 0.05$ ) or . ( $p < 0.10$ ).

Parameter	Tsoil p-value	N% p-value	Site p-value	Interaction p-value
Leaf C content	0.42	<b>&lt;0.001</b> ***	<b>0.02</b> *	0.91
$\delta^{13}\text{C}$	0.25	0.15	0.27	0.91
Leaf N content	0.25	/	0.98	0.63
$\delta^{15}\text{N}$	<b>0.09</b> .	0.63	0.70	0.23
Specific leaf area	0.77	0.28	0.68	0.56

The model excluding N-covariance showed that there were no significant impacts of Tsoil or site on C%, N%, stable isotopes or SLA. In the N-covariance model, the leaf C content was found to increase with increasing N% (+1.78% per %N, Table 8), which is not unexpected due to the strong N% effect on photosynthetic capacity parameters. Of the other parameters shown in Table 6 the  $\delta^{13}\text{C}$  is maybe of most interest. This value was not found to be significantly affected by Tsoil, site or N%, as it would if

drought (stomatal closures) would have been frequent in the warmer plots before the response curves were done in July.

An adaptation of plants to environmental conditions may not only be physiological or chemical but can also be morphological. The only morphological parameter tested in this study was SLA, which was not found to be significantly affected by any of the tested parameters (Tables 7 and 8).

## 4. Discussion

### 4.1 Effect of increasing soil temperature on photosynthesis

The first research question dealt with the impact of increasing soil temperature on photosynthesis in subarctic *R. acris*. The hypothesis was that plants growing in warmer plots exhibit higher assimilation rate. Many parameters, both in the survey and response curve measurements, showed no impact of soil temperature ( $T_{soil}$ ) as an individual variable, instead only showing significant differences in the interaction between site and  $T_{soil}$  – resulting in differences of parameters across  $T_{soil}$  in GO alone. These differences are mainly effects of site rather than  $T_{soil}$  and as such will be discussed in section 4.2.

In the model excluding N-covariance, no parameter showed a significant difference of  $T_{soil}$  (Table 4, Table 6). Only when examining the N-covariance model, some differences are visible, namely in  $C_i$  at  $C_a = 400$  ppm,  $\theta$  of the A/I response curve and LCP (Table 5). This suggests that these differences are mainly influenced by changes in leaf N content (N%). However, as N% did not differ significantly across  $T_{soil}$  (Table 7), the importance of these differences in regards to  $T_{soil}$  is limited.

Aside from their limited importance, the parameters that did show an impact of  $T_{soil}$  in the N-covariance model are contradictory to one another (Tables 4 and 5). Because of their limited importance, only one such contradiction will be discussed here as an example.  $C_i$  at  $C_a = 400$  ppm was lower in higher soil temperatures, suggesting one of two things; 1) that stomates are closed more often, indicating lower stomatal conductance, or 2) that assimilation rate (A at  $C_a = 400$  ppm) is higher, taking more C and converting it. Given that none of these two possibilities are present in the results, the relevance of the observation is unclear.

#### 4.1.1 Previous studies

In previous studies, the impact of warming on physiological plant parameters varied. Zhao & Liu (2012) showed a positive short-term warming effect on leaf N content,  $A_{max\_C_i}$  and AQY. Contradictorily, Loik et al. (2000) showed a negative effect of warming on AQY. Others, like the meta-analysis of Tibetan warming experiments by Fu et al. (2014), demonstrate an increase in specific leaf area, but no significant warming-induced differences in AQY,  $V_{c_{max}}$  or LSP. This large variety in results makes it difficult to discern a clear overarching effect of warming on photosynthetic parameters. It must be noted that the studies mentioned here are either air warming or combined air-soil warming experiments, which can partly explain differences with this study.

So then why is the expected warming impact as stated in the hypothesis not present in this research? One possible explanation could be that while warming may ameliorate certain photosynthetic processes, this increase can be counteracted by a decrease in nutrients. However, this hypothesis is contradicted by the result that reductions in leaf N content were not present in this case (Table 7).

Another explanation which may partially explain this lack of a clear temperature effect is the fact that while geothermal warming can heat soils up to 25°C above control, this heating effect is substantially lower in the canopy. While aboveground plant parts, among which leaves, are indirectly but crucially connected with plant parts in the soil, the temperature which is most influential for photosynthesis is not soil but leaf temperature. Unpublished data of Páll Sigurdsson showed that the increase of canopy temperature was limited to approx. 1-2°C in the e-plots and up to 4-5°C in extreme f-plots. However, despite the smaller temperature differences between a and e plots in the canopy than in the soil, clear differences were detected in the leaf metabolomes of plants grown in warmed versus control conditions. Earlier metabolome analyses of *R. acris* at the ForHot sites by Gargallo-Garriga et al. (2017) showed that the plant growing in warmer soils have distinctly different leaf metabolomic fingerprints (Fig. 22), most notably so in mechanisms pertaining to heat-shock reactions. This difference in metabolome points to profound differences in leaf function between leaves of plants growing in warmed versus unwarmed conditions, despite relatively small differences in canopy temperatures.

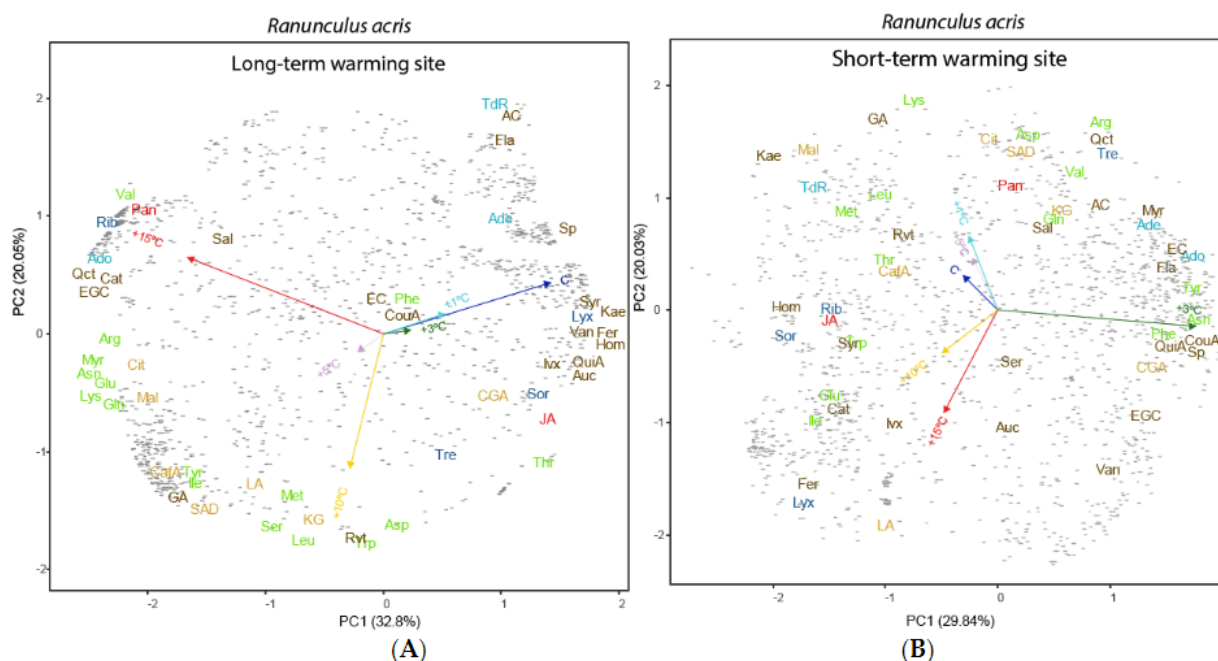


Fig. 22: Biplots of metabolome analysis of GO (a) and GN (b). The arrows indicate five different warming intensities. The two warming intensities corresponding to the plots investigated in this research are the blue (control; +0°C) and yellow arrows (warmed; +10°C). (Copied from Gargallo-Garriga et al., 2017)

Nonetheless, the lack of a clear impact of soil warming on photosynthetic mechanisms in this study – positive or negative – suggests that as ongoing climate warming persists, this warming will not lead to an increase or decrease in plant productivity.

#### 4.2 Effect of duration of soil warming on photosynthesis

The second research question focused on the impact of the duration of the warming, comparing medium-term (GN; 13 years) to long-term (GO; >60 years) soil warming. The hypothesis was that plants in long-term warmed plots have had more time to adjust to the warming and as such exhibit higher assimilation rate.

Many parameters showed a significant difference between sites and in interaction with  $T_{soil}$ , which results in differences between GN and GO as well as differences in slope between the two sites (Tables 3 and 4, Figs. 18 and 19). However, most of these parameters lose their significance when accounting for the covariance of N (Table 5). In other words, differences that appear to be between sites are actually caused by differences in leaf N content. As was the case when investigating the effect of soil temperature, the importance of these differences in regard to the effect of duration on soil warming is limited, as N% did not differ significantly between sites (Table 7). However, there were five parameters that retained their significance, regardless of inclusion of N-covariance. In the survey measurements,  $A_{net}$ ,  $A_{sat}$  and  $A_{max}$  differed significantly between sites. As for the response curve measurements, there were A at Ca = 400 ppm and LSP.

$A_{sat}$  and A at Ca = 400 ppm are linked, as they both show light-saturated photosynthesis at atmospheric  $CO_2$  concentration. Both parameters showed the same pattern: higher photosynthetic rate in GO at lower soil temperatures which decreased as the soil temperature got higher, while GN did not experience a difference in assimilation rate as soil temperature changed. These results are unexpected, as plants grown in long-term warmed soil were expected to have acclimated or adapted to this soil, whereas medium-term were expected not to.  $A_{net}$  and  $A_{max}$  showed the same trends. A possible explanation is that plants in GO have traded off some photosynthetic capacity in exchange for other traits that allowed them to function better in their warmed environment, a trade-off which plants in GN had not yet made. However, the fact that most other parameters did not show the same trends seems to dispute this hypothesis. Another possibility is that the weather conditions confounded the results of the survey measurements, a factor which  $A_{net}$  was especially susceptible to, as there was no standardisation of PAR or  $CO_2$ . A final explanatory factor may be that, as was the case in most other parameters, the leaf N content dictated largest part of the variation. The lack of sensitivity in these two important parameters to the experimental variables ( $T_{soil}$  and site) was an

important finding, as the maximum photosynthetic capacity was apparently not much affected by them, but more by variability in N status. This impact of N is discussed further in 4.3.

#### 4.2.1 Previous studies

As mentioned in the introduction, comparable studies looking into the long-term effects of soil warming on photosynthesis are rare. Perhaps the best source of research into long-term warming effects are earlier experiments within the ForHot project. One such experiment was a metabolomic analysis of *Ranunculus acris* and *Agrostis capillaris* by Gargallo-Garriga et al. (2017), which showed that the metabolome of *A. capillaris* clearly shifted at the site of long-term warming, while that of *R. acris* did not. On the other hand, *R. acris* metabolome did differ substantially in the short term at high soil warming, suggesting that *R. acris* plants adapted or acclimated their metabolism after long-term exposure to higher temperature, while *A. capillaris* did not.

This difference between long- and short-term warming at the ForHot site was also highlighted in Walker et al. (2020), who revealed a systemic overreaction in short-term warming. One of the causal factors mentioned was the short-lasting flush of excess nitrogen, released by a heat-driven increase in soil microbial activity in the years immediately following the earthquake. As plants in subarctic grasslands are accustomed to nutrient-low conditions, most of the excess nitrogen went unused and leached away or volatilised as NO<sub>x</sub>. In GN, where there is no subsoil, this leaching goes relatively fast (approx. 5-10 years), while the presence of subsoil in GO has the ability to store some of this excess nitrogen. The fact that there are little differences between sites, neither in photosynthetic properties nor in nutrient or carbon status, points towards the possibility that the systemic short-term overreaction as detailed in Walker et al., (2020) has come to pass and that GN too has already reached a new equilibrium.

*Ranunculus acris* plants growing in areas experiencing long-term sustained warming thus did not show increased photosynthetic capacities relative to those exposed to short-term warming. This implies that enhanced C uptake via warming-stimulated photosynthesis will not function as a buffer to retard global warming, as has been shown for the photosynthetic response to carbon pollution – the so-called carbon fertilisation effect (Erda et al., 2005; Matthews, 2007; Prentice et al., 2001).

### 4.3 Effect of plant nitrogen status

The most impactful factor throughout the measurements, more so than soil temperature or site, is leaf N concentration, which positively impacted many photosynthetic parameters (Table 5, Figs. 20

and 21). Nitrogen is a vital plant nutrient – especially important in photosynthesis. Approximately 75% of plant nitrogen is situated in the photosynthetic apparatus, especially in Rubisco (Larcher, 2003). In this capacity, many studies have demonstrated the positive impact of N-fertilisation on plant ecophysiology – and photosynthesis in particular (e.g. Zhao & Liu, 2012).

Given this context, it is not surprising that leaf nitrogen concentration positively influences many parameters in this study (Table 5). However, there was no difference in leaf N concentration between sites, nor across the soil temperature gradient (Table 7). It is therefore not possible to draw a clear line between the effect of warming, or duration thereof, and nitrogen status. The short-lasting flush excess N creating an effect of nitrogen fertilisation is interesting, but unfortunately confounds the direct warming effects. To better disentangle the warming from the nitrogen effects, two nitrogen addition experiments have been initiated at the ForHot sites.

#### 4.4 On the dynamicity of geothermal hotspots

While the geothermal field around Hveragerði is thought to have been stable for >60 years, in recent years a change has occurred. Geothermal activity is often dynamic in nature (Carotenuto et al., 2016) and the temporal variability in the geothermal activity is visible in two ways in the ForHot soil temperature data. The first is that over the past five years the temperature gradient in GN had increased – plots originally +20°C above control had increased to +26°C above control in 2021 – while the opposite was the case in GO – a decrease from +20°C above control originally to +8°C in 2021 (Fig. 6). The second striking example of geothermal dynamics was visible in the summer of 2021: as the temperature in the two warmest plots (e and f) in GN dropped by about 10°C over the span of just one day – August 23<sup>rd</sup>. A similar but less dramatic fall was seen in GO as well around the same date (Fig. 6). This drastic change can be explained by exceptionally dry conditions throughout 2021 (Icelandic Met Office, 2022) which resulted in less groundwater. This in turn effected an altered pressure on magma or perhaps caused less steam to reach to the surface. This experiment accounted for the actual soil temperatures and as such experienced no problems from the direct temperature effect. However, fluctuating temperature could influence the N cycle, which can affect plant functioning and photosynthesis over the course of multiple years. Thus it is important for this trend to remain under careful inspection in future projects.

#### 4.5 Limits of the project and discussion of different soil warming experiments

The potential of the ForHot in terms of warming experiments, as well as its publishing success, can hardly be overstated (e.g. Walker et al., 2018 and 2020). As mentioned earlier, however, photosynthesis – and other leaf- and other aboveground part-focussed studies – would do well with artificially increased air temperature in addition to the natural soil warming. This could be made possible with open-air chambers, which passively increase air temperature by trapping solar heat, as well as by creating a shelter against the wind (e.g. Marion et al., 1997). This type of passive warming can increase the temperature by a few degrees, but may be more effective than that in geothermal sites. Another possible method of actively creating air warming is by installing infrared lamps, as are used in the B4WarmED (Rich et al., 2015) and TeRaCON projects (Reich et al., 2020). An additional benefit of active warming is that the desired warming can be accurately applied. Both passive and active air warming would make the ForHot site an even better fitting proxy for climate change, especially in photosynthesis experiments.

Another expansion of the project would be the inclusion of drought treatment, nitrogen- and/or carbon dioxide-fertilisation. Nitrogen-fertilisation sites have already been set up in GN in 2016 and 2019 and could be made use of. Carbon fertilisation would more accurately reflect the reality of climate change and could be investigated in closed-top chambers or in free-air carbon enrichment (FACE) experiments (e.g. Reich et al., 2020). Unfortunately, due to the time consuming nature of response curve measurements, not all experiment expansion ideas can be examined simultaneously. In the context of the short-term excess N-flush as detailed by Walker et al. (2020), N-fertilisation could be interesting. In the broader context of climate change, however, drought and C-fertilisation experiments may provide more valuable knowledge. Finally, in order to get a full view of the subarctic grassland as an ecosystem, it may be a good idea to expand the study to the two other dominating species, *Agrostis capillaris* and *Equisetum pratense*.

#### 4.6 Importance for the future of the Arctic

Arctic and subarctic ecosystems have been presented as both a potential sink and source of future carbon (e.g. Bruhwiler et al., 2020; Miner et al., 2022). If the increase of plant production due to increased temperature and CO<sub>2</sub> outweighs the emission of soil carbon due to increased soil microbe activity following increased temperature, Arctic and subarctic ecosystems will act as a carbon sink. Unfortunately, the results of this study suggest that as global temperature rises, photosynthesis is likely not to follow suit. This will result in Arctic and subarctic ecosystems becoming sources of CO<sub>2</sub>.

## 5. Conclusion

As global warming is projected to continue throughout the century, it is important to understand how this will affect ecosystems throughout the world, but especially near the poles, where climate change is projected to have the greatest impact. Investigation into the effects of soil warming and the duration thereof on photosynthesis of *Ranunculus acris* in a subarctic grassland unexpectedly showed that there was little to no effect of soil temperature on photosynthetic parameters. While there were some differences between sites and thus duration of warming, most notably in maximal assimilation rate at saturating light and atmospheric carbon concentration, most of these differences were mainly explained by covariance of leaf nitrogen content. These results show that, as future soils warm up, increased plant productivity will not be able to offset the increase of emissions of soil carbon stocks. Future research into subarctic grasslands should look to include air warming in addition to soil warming. Furthermore, while this experiment investigated only warming, combined effects of carbon fertilisation or drought with warming could provide a more complete proxy for future global change.

## Acknowledgements

This project would not have been possible without the help and support of my mentor Ruth Phoebe Tchana Wandji, a PhD researcher within the FutureArctic program, and for that help I owe her many thanks. The value of Prof. dr. Bjarni D. Sigurdsson's expert knowledge, experience and guidance can also not be overstated. I would also like to thank prof. dr. Ivan A. Janssens for introducing me to the Icelandic project, as well as for giving key feedback throughout the writing process. Additionally, I would like to thank Páll Sigurðsson for his kindness as well as for the soil temperature data, Björn Ingi Stefánsson for his bond of friendship through shared intern experiences and all the other FutureArctic PhD students whom I got to meet and learn from throughout my months in Hveragerði. You deserve all the best!

## References

- Abdelrahman, M., Burritt, D. J., Gupta, A., Tsujimoto, H., & Tran, L.-S. P. (2020). Heat stress effects on source–sink relationships and metabolome dynamics in wheat. *Journal of Experimental Botany*, 71(2), 543–554.
- Bourdôt, G. W., Lamoureaux, S.L., Watt, M.S. & Kriticos, D.J. (2013). The Potential Global Distribution of Tall Buttercup (*Ranunculus acris*): Opposing Effects of Irrigation and Climate Change. *Weed Science*, 61(2), 230–238.
- Bruhwiller, L., Parmentier, F.-J. W., Crill, P., Leonard, M., & Palmer, P. I. (2021). The Arctic Carbon Cycle and Its Response to Changing Climate. *Current Climate Change Reports*, 7(1), 14–34.
- Carotenuto, A., Ciccolella, M., Massarotti, N., & Mauro, A. (2016). Models for thermo-fluid dynamic phenomena in low enthalpy geothermal energy systems: A review. *Renewable and Sustainable Energy Reviews*, 60, 330–355.
- Chen, C.T.A., Lui, H.K., Hsieh, C.H. et al. (2017). Deep oceans may acidify faster than anticipated due to global warming. *Nature Clim Change* 7, 890–894.
- Colucci, R.R., Guglielmin, M. (2019). Climate change and rapid ice melt: Suggestions from abrupt permafrost degradation and ice melting in an alpine ice cave. *Progress in Physical Geography: Earth and Environment* 43, 561–573.
- De Gruyter, J., Weedon, J. T., Bazot, S., Dauwe, S., Fernandez-Garberí, P.-R., Geisen, S., Louis Gourlez, Heinesch, B., Janssens, I. A., Leblans, N., Manise, T., Ogaya, R., Löfvenius, M. O., Peñuelas, J., Sigurdsson, B. D., Vincent, G., & Verbruggen, E. (2020). Patterns of local, intercontinental and interseasonal variation of soil bacterial and eukaryotic microbial communities. *FEMS Microbiology Ecology*, 96(3).
- Dieleman, W. I. J., Vicca, S., Dijkstra, F. A., Hagedorn, F., Hovenden, M. J., Larsen, K. S., Morgan, J. A., Volder, A., Beier, C., Dukes, J. S., King, J., Leuzinger, S., Linder, S., Luo, Y., Oren, R., De Angelis, P., Tingey, D., Hoosbeek, M. R., & Janssens, I. A. (2012). Simple additive effects are rare: a quantitative review of plant biomass and soil process responses to combined manipulations of CO<sub>2</sub> and temperature. *Global Change Biology*, 18(9), 2681–2693.
- Duursma, R. A. (2015). Plantecophys - An R Package for Analysing and Modelling Leaf Gas Exchange Data. *PLOS ONE*, 10(11), e0143346.
- Erda, L., Wei, X., Hui, J., Yinlong, X., Yue, L., Liping, B. & Liyong, X. (2005). Climate change impacts on crop yield and quality with CO<sub>2</sub> fertilization in China. *Phil. Trans. R. Soc. B: Biological Sciences*, 360(1463), 2149–2154.
- Farquhar, G. D., Von Caemmerer, S., & Berry, J. A. (1980). A biochemical model of photosynthetic CO<sub>2</sub> assimilation in leaves of C<sub>3</sub> species. *Planta*, 149(1), 78–90.

- Fassioli, F., Dinshaw, R., Arpin, P.C., Scholes, G.D. (2014). Photosynthetic light harvesting: excitons and coherence. *Journal of The Royal Society Interface* 11, 20130901.
- Fdz-Polanco, F., Villaverde, S. & García, P. A. (1994). Temperature effect on nitrifying bacteria activity in biofilters: activation and free ammonia inhibition. *Water Science and Technology*, 30(11), 121–130.
- Fu, G., Shen, Z.-X., Sun, W., Zhong, Z.-M., Zhang, X.-Z., & Zhou, Y.-T. (2014). A Meta-analysis of the Effects of Experimental Warming on Plant Physiology and Growth on the Tibetan Plateau. *Journal of Plant Growth Regulation*, 34(1), 57–65.
- Gargallo-Garriga, A., Ayala-Roque, M., Sardans, J., Bartrons, M., Granda, V., Sigurdsson, B., Leblans, N., Oravec, M., Urban, O., Janssens, I., Peñuelas, J. (2017). Impact of Soil Warming on the Plant Metabolome of Icelandic Grasslands. *Metabolites* 7, 44.
- Gargallo-Garriga, A., Sardans, J., Ayala-Roque, M., Sigurdsson, B. D., Leblans, N. I. W., Oravec, M., Klem, K., Janssens, I. A., Urban, O., & Peñuelas, J. (2021). Warming affects soil metabolome: The case study of Icelandic grasslands. *European Journal of Soil Biology*, 105, 103317.
- Halldórsson, B., & Sigbjörnsson, R. (2009). The Ölfus earthquake at 15:45 UTC on 29 May 2008 in South Iceland: ICEARRAY strong-motion recordings. *Soil Dynamics and Earthquake Engineering*, 29(6), 1073–1083.
- Hawkes, C.V., Hartley, I.P., Ineson, P & Fitter, A.H. (2007). Soil temperature affects carbon allocation within arbuscular mycorrhizal networks and carbon transport from plant to fungus. *Global Change Biology* 14, 1181-1190.
- Heberling, J.M. (2014). A practical guide to measuring leaf-level photosynthesis. Fridley lab: [https://sites.google.com/site/fridleylab/home/protocols/Heberling\\_PhotosynthesisProtocol\\_Feb2014.pdf?attredirects=0](https://sites.google.com/site/fridleylab/home/protocols/Heberling_PhotosynthesisProtocol_Feb2014.pdf?attredirects=0)
- Heckmann, D., Schulze, S., Denton, A., Gowik, U., Westhoff, P., Andreas, & Martin. (2013). Predicting C4 Photosynthesis Evolution: Modular, Individually Adaptive Steps on a Mount Fuji Fitness Landscape. *Cell*, 153(7), 1579–1588.
- Huang, B., Rachmilevitch, S., & Xu, J. (2012). Root carbon and protein metabolism associated with heat tolerance. *Journal of Experimental Botany*, 63(9), 3455–3465.
- IPCC (2021). Summary for Policymakers. In: *Climate Change 2021: The Physical Science Basis. Contribution of Working Group I to the Sixth Assessment Report of the Intergovernmental Panel on Climate Change* [Masson-Delmotte, V., P. Zhai, A. Pirani, S.L. Connors, C. Péan, S. Berger, N. Caud, Y. Chen, L. Goldfarb, M.I. Gomis, M. Huang, K. Leitzell, E. Lonnoy, J.B.R. Matthews, T.K. Maycock, T. Waterfield, O. Yelekçi, R. Yu, and B. Zhou (eds.)]. Cambridge University Press, Cambridge, United Kingdom and New York, NY, USA, pp. 3–32.

- IPCC (2022). Summary for Policymakers. In: *Climate Change 2022: Mitigation of Climate Change. Contribution of Working Group III to the Sixth Assessment Report (AR6) of the Intergovernmental Panel on Climate Change*. Cambridge University Press, Cambridge, United Kingdom and New York, NY, USA, pp. 3–32.
- Jamieson, M.A., Schwartzberg, E.G., Raffa, K.F., Reich, P.B., Lindroth, R.L., 2015. Experimental climate warming alters aspen and birch phytochemistry and performance traits for an outbreak insect herbivore. *Global Change Biology* 21, 2698–2710.
- Jansson, J.K. & Hofmockel, K.S. (2019). Soil microbiomes and climate change. *Nat. Rev. Microbiol.* 18, 35–46.
- Kuhlbrodt, T., Gregory, J.M. (2012). Ocean heat uptake and its consequences for the magnitude of sea level rise and climate change. *Geophysical Research Letters* 39.
- Kutcherov, D., Slotsbo, S., Sigurdsson, B. D., Leblans, N. I. W., Berg, M. P., Ellers, J., Mariën, J., & Holmstrup, M. (2020). Temperature responses in a subarctic springtail from two geothermally warmed habitats. *Pedobiologia*, 78, 150606.
- Lambers, H., Chapin III, F.S. & Pons, T.L. 1998. *Plants Physiological Ecology*. Springer-Verlag New York, Inc: 540.
- Larcher, W. (2003). *Physiological Plant Ecology*, Fourth Edition. Germany: Springer-Verlag Berlin Heidelberg.
- Leblans, N. I. W., Sigurdsson, B. D., Vicca, S., Fu, Y., Penuelas, J., & Janssens, I. A. (2017). Phenological responses of Icelandic subarctic grasslands to short-term and long-term natural soil warming. *Global Change Biology*, 23(11), 4932–4945.
- Lensen, N., G. Schmidt, J. Hansen, M. Menne, A. Persin, R. Ruedy, and D. Zyss, (2019). Improvements in the GISTEMP uncertainty model. *J. Geophys. Res. Atmos.*, 124, 6307-6326.
- Loik, M. E., Redar, S. P., & Harte, J. (2000). Photosynthetic responses to a climate-warming manipulation for contrasting meadow species in the Rocky Mountains, Colorado, USA. *Functional Ecology*, 14(2), 166–175.
- Marion, G. M., Henry, G. H. R., Freckman, D. W., Johnstone, J., Jones, G., Jones, M. H., Lévesque, E., Molau, U., Mølgaard, P., Parsons, A. N., J. Svoboda, & Virginia, R. A. (1997). Open-top designs for manipulating field temperature in high-latitude ecosystems. *Global Change Biology*, 3(S1), 20–32.
- Matesanz, S., Valladares, F., 2014. Ecological and evolutionary responses of Mediterranean plants to global change. *Environmental and Experimental Botany* 103, 53–67.
- Matthews, H. D. (2007). Implications of CO<sub>2</sub> fertilization for future climate change in a coupled climate carbon model. *Global Change Biology*, 13(5), 1068–1078.

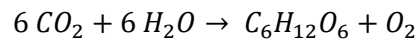
- McPartland, M.Y., Montgomery, R.A., Hanson, P.J., Phillips, J.R., Kolka, R. and Palik, B. (2020). Vascular plant species response to warming and elevated carbon dioxide in a boreal peatland. *Environ. Res. Lett.* 15, 124066.
- Meinshausen, M., Meinshausen, N., Hare, W., Raper, S. C. B., Frieler, K., Knutti, R., Frame, D. J. & Allen, M. (2009) Greenhouse gas emission targets for limiting global warming to 2°C. *Nature*, 458: 1158-1163.
- Miner, K.R., Tretsky, R.T., Malina, E., Bartsch, A., Tamminen, J., McGuire, A.D., Fix, A., Sweeney, C., Elder, C.D. & Miller, C.E. (2022). Permafrost carbon emissions in a changing Arctic. *Nature Reviews Earth & Environment* 3, 55–67.
- Nelson, D.L. & Cox, M.M. (2013). *Lehninger Principles of Biochemistry*, Sixth Edition. New York: W. H. Freeman and Company.
- Nóia Júnior, R. D. S., Do Amaral, G. C., Pezzopane, J. E. M., Toledo, J. V., & Xavier, T. M. T. (2018). Ecophysiology of C3 and C4 plants in terms of responses to extreme soil temperatures. *Theoretical and Experimental Plant Physiology*, 30(3), 261–274.
- Prentice, I.C., Farquhar, G.D., Fasham, M.J.R., Goulden, M.L., Heimann, M., et al. (2001). The carbon cycle and atmospheric carbon dioxide. Intergovernmental panel on climate change, *Climate change 2001: the scientific basis*.
- Reich, P.B., Hobbie, S.E., Lee, T.D., Rich, R., Pastore, M.A. and Worm, K. (2020). Synergistic effects of four climate change drivers on terrestrial carbon cycling. *Nature Geoscience*, 13, 787-793.
- Rich, R. L., Stefanski, A., Montgomery, R.A., Hobbie, S.E.; Kimball, B.A. & Reich, P.B. (2015). Design and performance of combined infrared canopy and belowground warming in the B4WarmED (Boreal Forest Warming at an Ecotone in Danger) experiment. *Global Change Biology*, 21(6), 2334–2348.
- Roberntz, P., & Stockfors, J. (1998). Effects of elevated CO<sub>2</sub> concentration and nutrition on net photosynthesis, stomatal conductance and needle respiration of field-grown Norway spruce trees. *Tree Physiology*, 18(4).
- Sarukhan, J., & Gadgil, M. (1974). Studies on Plant Demography: *Ranunculus Repens* L., *R. Bulbosus* L. and *R. Acris* L.: III. A Mathematical Model Incorporating Multiple Modes of Reproduction. *Journal of Ecology*, 62(3), 921.
- Sharp, M., Burgess, D.O., Cogley, J.G., Ecclestone, M., Labine, C., Wolken, G.J. (2011). Extreme melt on Canada's Arctic ice caps in the 21st century. *Geophysical Research Letters* 38
- Sigurdsson, B.D., Leblans, N.I.W., Dauwe, S., Guðmundsdóttir, E., Gundersen, P., Gunnarsdóttir, G. E., Holmstrup, M., Ilieva-Makulec, K., Janssens, I. (2016) Geothermal ecosystems as natural

- climate change experiments: the ForHot research site in Iceland as a case study, *Icel. Agric. Sci.* 29 53–71.
- Sigurdsson, D.B., Roberntz, P., Freeman, M., Naess, M., Saxe, H., Thorgeirsson, H. & Linder, S. (2002). Impact studies on Nordic forests: effects of elevated CO<sub>2</sub> and fertilization on gas exchange. *Can. J. For. Res.* 32, 779-788.
- Stott, P. (2016). How climate change affects extreme weather events. *Science* 352, 1517-1518.
- Þorbjörnsson, D., Sæmundsson, K., Kristinsson, S.G., Kristjánsson, B.R. & Ágústsson, K. (2009). Suðurlandskjálftar 29. maí 2008. Áhrif á grunnvatnsborð, hveravirkni og sprungumyndun [The South Iceland earthquake on 29th of May 2008. Impacts on groundwater levels, activity of geothermal hot-spots and creation of seismic cracks]. Rep. No. ÍSOR-2009/028. Unnið fyrir Orkuveitu Reykjavíkur, Iceland Geosurvey, Reykjavik, Iceland, 42 p. [In Icelandic]
- Van Oldenborgh, G.J., Drijfhout, S., Van Ulden, A., Haarsma, R., Sterl, A., Severijns, C., Hazeleger, W., Dijkstra, H. (2009). Western Europe is warming much faster than expected. *Climate of the Past* 5, 1–12.
- Verlinden, M. S., Abdelgawad, H., Ven, A., Verryckt, L. T., Wieneke, S., Janssens, I. A., & Vicca, S. (2022). Phosphorus stress strongly reduced plant physiological activity, but only temporarily, in a mesocosm experiment with *Zea mays* colonized by arbuscular mycorrhizal fungi. *Biogeosciences*, 19(9), 2353–2364.
- Walker, T. W. N., Janssens, I. A., Weedon, J. T., Sigurdsson, B. D., Richter, A., Peñuelas, J., Leblans, N. I. W., Bahn, M., Bartrons, M., De Jonge, C., Fuchslueger, L., Gargallo-Garriga, A., Gunnarsdóttir, G. E., Marañón-Jiménez, S., Oddsdóttir, E. S., Ostonen, I., Poeplau, C., Prommer, J., Radujković, D., ... Verbruggen, E. (2020). A systemic overreaction to years versus decades of warming in a subarctic grassland ecosystem. *Nature Ecology & Evolution*, 4(1), 101–108.
- Walker, T. W. N., Kaiser, C., Strasser, F., Herbold, C. W., Leblans, N. I. W., Woebken, D., Janssens, I. A., Sigurdsson, B. D., & Richter, A. (2018). Microbial temperature sensitivity and biomass change explain soil carbon loss with warming. *Nat. Clim. Chang.*, 8(10), 885–889.
- Wang, S. Duan, J. Xu, G., Wang, Y., Zhang, Z., Rui, Y., Luo, C., Xu, B., Zhu, X., Chang, X., Cui, X., Niu, H., Zhao, X. & Wang, W. (2012). Effects of warming and grazing on soil N availability, species composition, and ANPP in an alpine meadow. *Ecology* 93, 2365-2376.
- Wullschleger, S.D. (1993). Biochemical Limitations to Carbon Assimilation in C<sub>3</sub> Plants—A Retrospective Analysis of the A/Ci Curves from 109 Species. *Journal of Experimental Botany*, 44(5), 907–920.
- Xu, Y., Ramanathan, V. & Victor, D.G. (2018). Global warming will happen faster than we think. *Nature* 564, 30-32.

- Yamori, W., Hikosaka, K., Way, D.A., (2014). Temperature response of photosynthesis in C3, C4, and CAM plants: temperature acclimation and temperature adaptation. *Photosynthesis Research* 119, 101–117.
- Zakharova, O. K., & Spichak, V. V. (2012). Geothermal fields of Hengill Volcano, Iceland. *Journal of Volcanology and Seismology*, 6(1), 1–14.
- Zhao, C., & Liu, Q. (2012). Effects of soil warming and nitrogen fertilization on leaf physiology of *Pinus tabulaeformis* seedlings. *Acta Physiologiae Plantarum*, 34(5), 1837–1846.

## Addendum 1: Theory on photosynthesis

Photosynthesis is the biochemical mechanism through which plants convert light energy into chemical energy by turning carbon dioxide (CO<sub>2</sub>) along with water into carbohydrates following the general (simplified) formula:



This process occurs in the chloroplasts in green structures in plants. Most of the chloroplasts are concentrated in the leaves, which act as specialised structures for gas exchange (Lambert et al., 1998).

The reality of photosynthesis is slightly more complicated than the above formula suggests, consisting of two main steps: light dependent reactions and light independent reactions.

### Light dependent reactions

The first step in converting energetically stable CO<sub>2</sub> into energy rich carbohydrates is capturing sunlight. This light absorption in chloroplasts occurs mainly in chlorophyll pigments (*chl a* and *chl b*), capturing chiefly blue (380-500 nm) and red light (600-700 nm). Green light is not absorbed as much and is as such reflected, giving the leaves their green colour. Besides chlorophyll, light is absorbed in lesser degrees by accessory pigments such as carotenes ( $\beta$ -carotene and lutein), phycocyanin and phycoerythrin, slightly expanding the absorbed spectrum (Fig. 23).

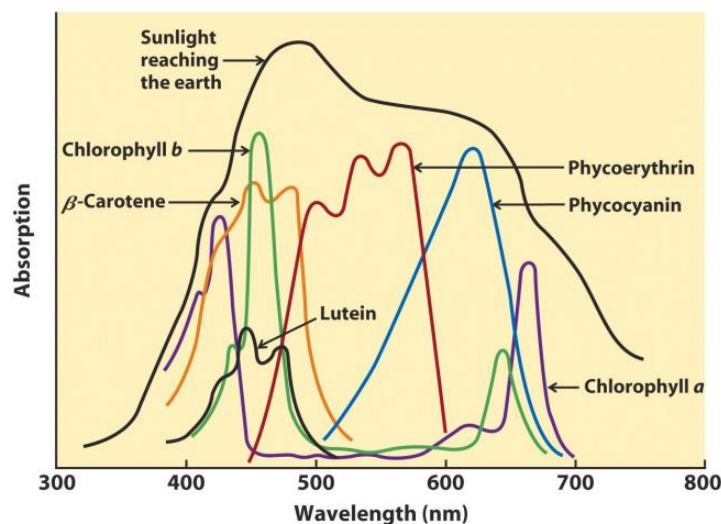


Fig. 23: Spectrum of incident sunlight (black) and the absorption of photosynthetic pigments: *chl a* (purple), *chl b* (green) and accessory pigments (other colours). (Nelson & Cox, 2013)

These photosynthetic pigments are aggregated in photosystems (PSII and PSI) and connected with so-called light harvesting complexes (LHCs), which are embedded in the thylakoid membranes. In these complexes, light is absorbed by antenna molecules (mostly *chl b* and carotenes) and transferred to the photochemical reaction centre through exciton transfer (Fassioli et al., 2014). In this reaction centre, the transferred photosynthetically active radiation (PAR) stimulates a dimer of *chl a* to photolyse water, releasing electrons. These electrons then get transported through the two photosystems, adding to a proton gradient and reducing  $NADP^+$  to NADPH. The resulting proton build-up in the thylakoid lumen then powers ATP synthase, a protein pump which converts ADP into ATP (Larcher, 2003).

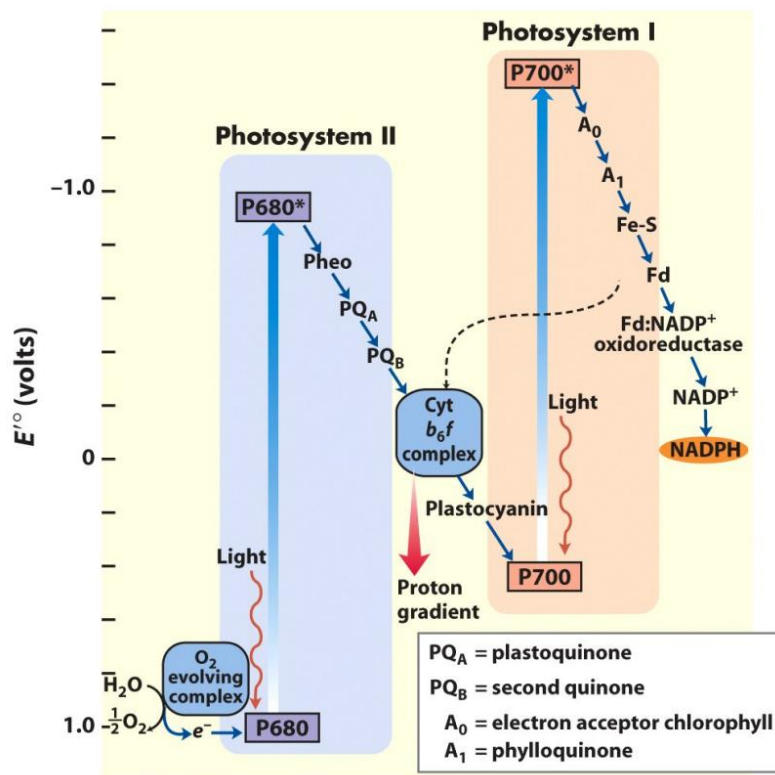
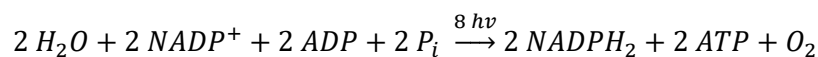


Fig. 24: Z-scheme. Energy diagram of the electron transport of PSII and PSI in light dependent reactions. (Nelson & Cox, 2013)

This photochemical process can be summarised in the following formula (Larcher, 2003):



## Light independent reactions

The energy and reducing power produced in the light dependent reactions is used to reduce  $\text{CO}_2$  into carbohydrates in several steps in the light independent reactions, also known as the Calvin cycle (Fig. 25). In the first step,  $\text{CO}_2$  entering the chloroplast is bound to an acceptor, RuBP, which then undergoes carboxylation catalysed by the enzyme Rubisco. The carboxylation product, a six-carbon molecule, decomposes immediately to produce two molecules both containing 3 carbon atoms. These three-carbon-containing molecules are the reason this process is also called the  $\text{C}_3$  assimilation pathway. These molecules are reduced over several steps into carbohydrates of various carbon chain length ( $\text{C}_3$ - $\text{C}_7$ ) from which various substances such as glucose, starch and amino acids are synthesised. The acceptors are then regenerated (Larcher, 2003).

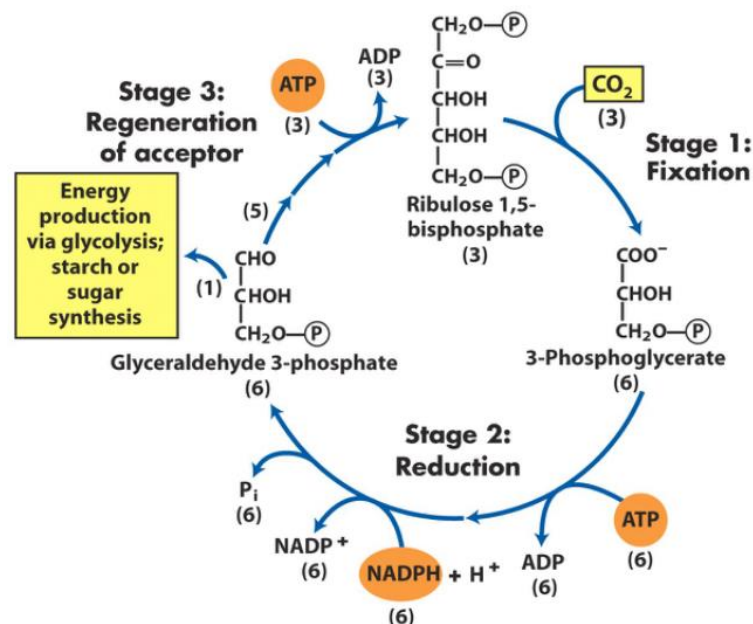


Fig. 25: The Calvin cycle with three steps: Stage 1, fixation of  $\text{CO}_2$ ; Stage 2, reduction of 3-phosphoglycerate to glyceraldehyde 3-phosphate; Stage 3, regeneration of acceptor RuBP. (Nelson & Cox, 2013)

Finally, Larcher (2003) has this to say about carboxylation efficiency:

The *carboxylation efficiency*, i.e. the speed by which  $\text{CO}_2$  is processed after its uptake, is mostly limited by the quantity and activity of the enzyme and the availability of  $\text{CO}_2$ . Other factors influencing carboxylation efficiency are acceptor concentration, leaf temperature, the degree of hydration of the protoplasm, the supply of minerals and the stage of development and stage of activity of the plant

## Addendum 2: graphs

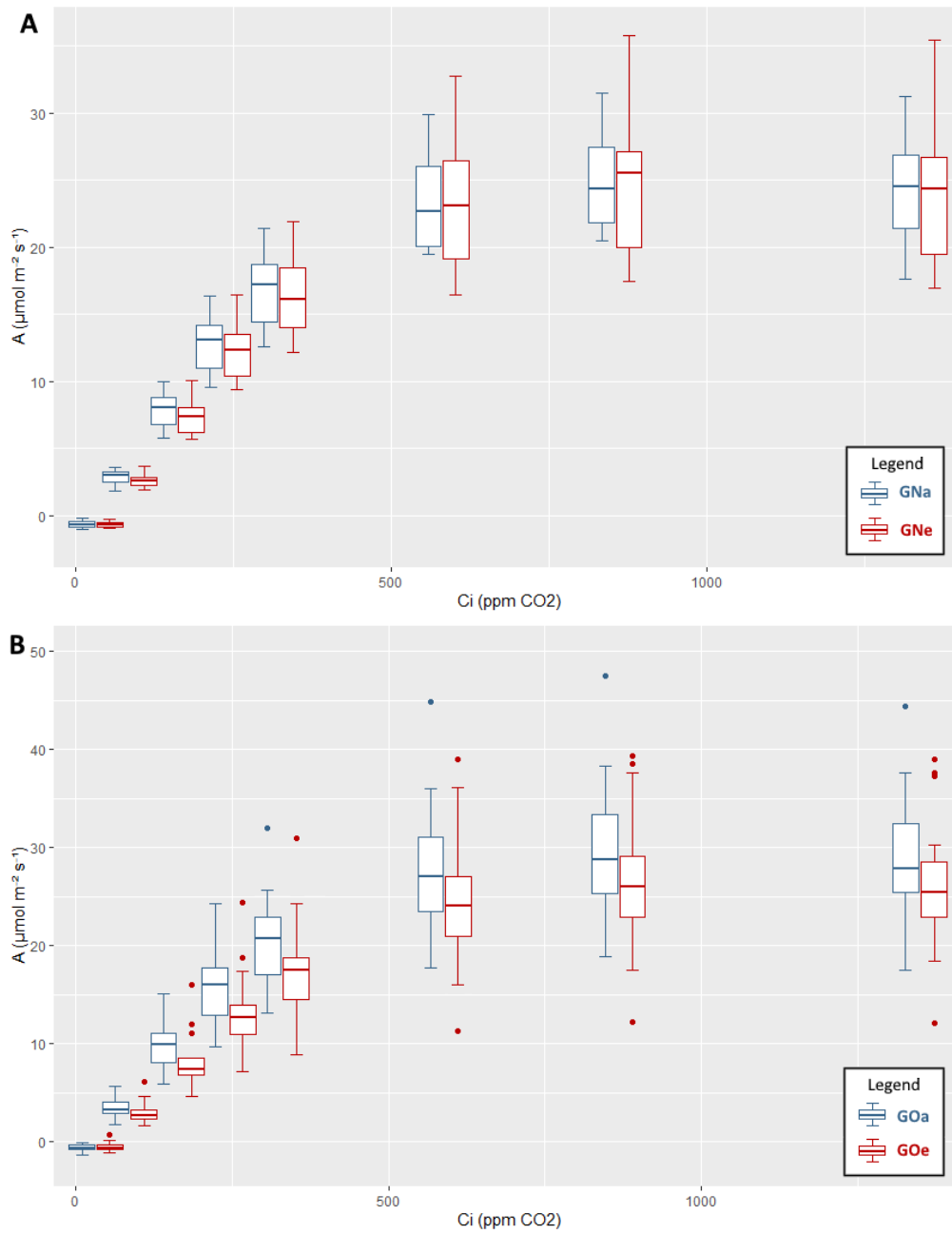


Fig. 26: Boxplot summaries of all  $A/C_i$  measurements for GN (a) and GO (b) ( $n = 12$  and  $n = 15$ , respectively). Control plots in blue, warmed plots in red.

## Addendum 3: Survey measurement protocol

By Timon Callebaut, 03/09/2021

### Starting up the LiCOR 6800

- Before starting the console: attach head, CO<sub>2</sub> cannister and columns (H<sub>2</sub>O desiccant and humidifier & CO<sub>2</sub> desiccant).
  - **Warning:** Soda lime (CO<sub>2</sub> scrub column) causes **severe burns when wet**. Wear suitable gloves and eye and face protection. Keep out of reach of children. In case of contact with eyes, rinse immediately with plenty of water and seek medical advice.
- Start the console.
- Under 'Startup' -> 'Warmup/system tests', run the Warmup/system tests
  - Errors need to be fixed (follow instructions of the LiCOR)
  - Warnings should be looked at, decide for yourself how to proceed (usually following the instructions and then starting your measurements is fine)

### Measurements

#### Settings

Under 'Environment', set followings settings to:

- Flow: 600
  - Can be raised if the chamber is close to reaching condensation point (100% RH). Keep in mind that this change may impact boundary layer conductance.
- H<sub>2</sub>O: VPD = 1.1
- CO<sub>2</sub>: 30
- Fan: 10000
- Temperature: T<sub>air</sub> (or T<sub>leaf</sub>) = 20
- Light: set light similar to ambient light

IRGA matching: acquire point match at 400 and 1000 ppm CO<sub>2</sub> (faster) or take range matching (slower)

- Retake matching upon changes in ambient & chamber temperature

#### Measurements

1. Clamp leaf in chamber
  - Preferably mature, healthy leaves
2. Wait for stabilisation of g<sub>sw</sub> (if you're interested in stomatal conductance), log four measurements
3. Wait for stabilisation of A, log four measurements
4. Change light to 2000
5. Wait for stabilisation, log four measurements (=A<sub>sat</sub>)
6. Change CO<sub>2</sub> to 1000

7. Wait for stabilisation, log four measurements ( $=A_{\max}$ )

### Post-response curve

- Assuming the leaf didn't fill the entire chamber, you need to recalculate the values of every surface area-based parameter with the correct leaf area size.
  - To do this, collect the parts of the leaf & stem that were **inside of the chamber**.
  - Obtain the surface area of the used leaf by scanning (ask Bjarni) or using other methods (e.g. ImageJ)
  - Change the surface area in the Excel datafile, which can be found under Constants -> S (cell B6 in version 1.4). Upon doing this, the values should change automatically.
- Leaf can be used for other relevant tests (e.g. nutrient analysis)
  - Store in freezer (e.g.  $-20^{\circ}\text{C}$ ) until further analysis

## Addendum 4: Response curve protocol

By Timon Callebaut, 19/08/2021

### Starting up the LiCOR 6800

- Before starting the console: attach head, CO<sub>2</sub> cannister and columns (H<sub>2</sub>O desiccant and humidifier & CO<sub>2</sub> desiccant).
  - **Warning:** Soda lime (CO<sub>2</sub> scrub column) causes **severe burns when wet**. Wear suitable gloves and eye and face protection. Keep out of reach of children. In case of contact with eyes, rinse immediately with plenty of water and seek medical advice.
- Start the console.
- Under 'Startup' -> 'Warmup/system tests', run the Warmup/system tests
  - Errors need to be fixed (follow instructions of the LiCOR)
  - Warnings should be looked at, decide for yourself how to proceed (usually following the instructions and then starting your measurements is fine)

### Response curves

#### A/Ci response curve

8. Under 'Environment', set followings settings to:
  - Flow: 600
    - Can be raised if the chamber is close to reaching condensation point (100% RH). Keep in mind that this change may impact boundary layer conductance.
  - H<sub>2</sub>O: VPD = 1.1
  - CO<sub>2</sub>: 30
  - Fan: 10000
  - Temperature: T<sub>air</sub> (or T<sub>leaf</sub>) = 20
  - Light: 2000
9. **Range matching:** go to measurements -> match IRGAs -> match CO<sub>2</sub> -> acquire
  - Also do H<sub>2</sub>O
  - Retake matching upon changes in ambient & chamber temperature
10. Clamp leaf in chamber
  - Preferably mature, healthy leaves
11. Wait for stabilisation
12. Log four measurements
13. Change CO<sub>2</sub> to next level

- To make comprehensive A/Ci response curves, consider taking as many CO<sub>2</sub> levels as necessary. When unsure, start with ten points, for example: 30, 100, 200, 300, 400, 500, 700, 1000, 1200 & 1500.
    - The lowest CO<sub>2</sub> level should be below the respiration compensation point. (LICOR recommends 30 for C<sub>3</sub>-plants and 0 for C<sub>4</sub>-plants)
  - Taking ten points is not always necessary: review the curves to leave away unnecessary points.
14. Repeat steps 3-5.
15. After taking the last measurement, it is possible to go immediately into A/I response curves

### A/I response curve

1. Change PAR to next level, leave other parameters unchanged.
  - If you've taken A/Ci curve immediately before this, you can skip taking the max CO<sub>2</sub>/max PAR measurement, as it has already been taken in the A/Ci measurements.
  - To make comprehensive A/I response curves, consider taking as many PAR levels as necessary. When unsure, start with ten points, for example: 0, 50, 100, 250, 500, 750, 1000, 1250, 1500 & 2000.
  - Taking ten points is not always necessary. Review the curves to leave away unnecessary points.
2. Wait for stabilisation
3. Log four measurements
4. Change PAR to next level
5. Repeat steps 2-4.

### Post-response curve

- Assuming the leaf didn't fill the entire chamber, you need to recalculate the A, E and every other surface area-based parameter with the correct leaf area size.
  - To do this, collect the parts of the leaf & stem that were **inside of the chamber**.
  - Obtain the surface area of the used leaf by scanning (ask Bjarni) or using other methods (e.g. ImageJ)
  - Change the surface area in the Excel datafile, which can be found under Constants -> S (cell B6 in version 1.4). Upon doing this, the values should change automatically.
- Leaf can be used for other relevant tests (e.g. nutrient analysis)
  - Store in freezer (e.g. -20°C) until further analysis

### Additional notes

- Bring the backup battery (because of the high light blasted at the plants, response curves require lots of energy)
- Stabilisation can take 4-6 minutes, so be patient.